1-1-2014

Bystander Effects Due To Neutrons, And Low-Dose Hyper-Radiosensitivity To Gamma Rays In Human Cells Using Cytogenetics

Isheeta Seth
Wayne State University,

BYSTANDER EFFECTS DUE TO NEUTRONS, AND LOW-DOSE HYPER-RADIOSENSITIVITY TO GAMMA RAYS IN HUMAN CELLS USING CYTOGENETICS

by

ISHEETA SETH

DISSERTATION

Submitted to the Graduate School

of Wayne State University,

Detroit, Michigan

in partial fulfillment of the requirements

for the degree of

DOCTOR OF PHILOSOPHY

2014

MAJOR: BIOLOGICAL SCIENCES

Approved by:

_____

Advisor Date

_____

_____

_____

_____

DEDICATION

I want to dedicate this work to my parents: Gaggan Seth and Saroj Seth, my elder sister: Ipsa Seth, my late maternal grandparents: Raj Kumari Khanna and C.L. Khanna, and my late paternal grandparents: Santosh Seth and Raj Kumar Seth. None of this would have been possible without their blessings, unconditional love, support and immense faith in me.

ACKNOWLEDGEMENTS

To come halfway across the world to pursue a PhD was definitely one of the biggest decisions I took in my life and it has been the best one so far. My scientific journey would not have been so great without the support and guidance from some wonderful and knowledgeable people whom I interacted with and learned from over the past 5 years.

First and foremost, I feel extremely blessed to have had the opportunity to work with the most amazing advisor: Dr. James D. Tucker. I cannot imagine of a mentor as perfect and motivating as he is. He has been a constant source of support, positivity and patience in every situation during my PhD. He is always very supportive, fair and respectful to his graduate students and has been extraordinarily successful in maintaining a positive and a healthy environment in a laboratory full of culturally diverse people. He saw the potential in me when I couldn't and helped me bring out the best in me. He never tried to impose his opinions on me, instead, he always patiently listened to my thoughts and ideas first, and helped me groom scientifically and develop my own style. Thank you so much Dr. Tucker for making me believe in myself, for giving me the confidence to pursue my goals, and for equipping me with a variety of technical as well as interpersonal skills. I will always owe a huge part of my success in my future scientific career to you.

The one thing that made the Tucker lab so different and a fun place to work was the opportunity to interview, recruit and train undergraduate students. I got a chance to work with seven most outstanding undergraduate students who assisted me with

microscopy. Thank you Umair Waheed, Marcy Johnston, Mary Abu-farah, Ahmad Suleiman, Sergiy Boyco, Slavica Gjorgjevska and Zainab Hammoud. None of my projects would have completed timely without them, especially Zainab Hammoud who was exceptionally smart and always available when needed. I also want to thank Dr. Robert A. Thomas for all his inspiring words and appreciation whenever I met him.

I want to thank my PhD committee members: Dr. Michael C. Joiner, Dr. Victoria Meller and Dr. Xiang-Dong Zhang who were always available to me whenever I needed their advice. Their valuable comments and suggestions helped me to be on track and consistently progress through my PhD. None of my projects would have even been initiated had it not been for Dr. Joiner's help in performing all the radiation exposures. Despite his extremely busy schedule, he managed to fit in my radiation schedules very efficiently and made sure all my experiments were executed and completed timely.

I was lucky to get an awesome group of collaborators and co-authors in University of Washington Medical Center (UWMC) for my fast neutron work. I want to thank Dr. Jeffrey L. Schwartz, Dr. Robert D. Stewart and Dr. Robert Emery for being so cooperative. Without them there was no way I could have done my neutron studies. I also want to thank Geoffrey Linn (technician in Dr. Schwartz's lab) for his technical support and for helping me settle down in the lab during my visit to UWMC.

I want to thank the past and current Tucker lab members: Han Cheong (also a joint co-author), Marina Bakhmutsky and Gnanada Joshi for their friendship and all the fun times we have shared. I know they are always there for me whenever I need someone with whom to share my happiness or sorrow. I want to thank the staff of the

Biological Sciences Department especially Rose Mary P. Priest, Louise Dezur and my graduate school advisor Dr. Edward Golenberg for taking care of all the PhD paper work and giving timely reminders, making a student's life much simpler. I also want to thank the funding support by the Wayne State University Graduate Enhancement Research Funds and the Rumble fellowship.

My family and friends have always been my strength and very supportive of my goals and dreams. Nothing gave me as much motivation to keep going as my dad's inspiring words, my mom's care and my sister's love. I also want to thank my cousin: Souful Bhatia who motivated me to apply to the US and Aman Sangwan who is always there for me as a friend and a mentor. A special thanks to my aunt and uncle: Bina Kapoor and Virender Kapoor in Alabama who provided me with all the emotional care and support I needed being away from home. Last but not the least, none of this would be possible without the blessings and will of the Almighty.

TABLE OF CONTENTS

LIST OF TABLES

LIST OF FIGURES

CHAPTER 1

INTRODUCTION

Ionizing Radiation

Ionizing radiation (IR) is a type of energy or particle that can remove tightly bound electrons from the orbit of atoms and cause them to become charged or ionized. IR can lead to chromosome damage causing cancer, yet IR is also used for treating tumors because of its ability to kill cells by inducing DNA double strand breaks. Four of the most commonly evaluated types of IR are alpha particles, beta particles, photons (gamma and x-rays), and fast neutrons. Figure 1.1 indicates the penetrating powers of these four radiation types.

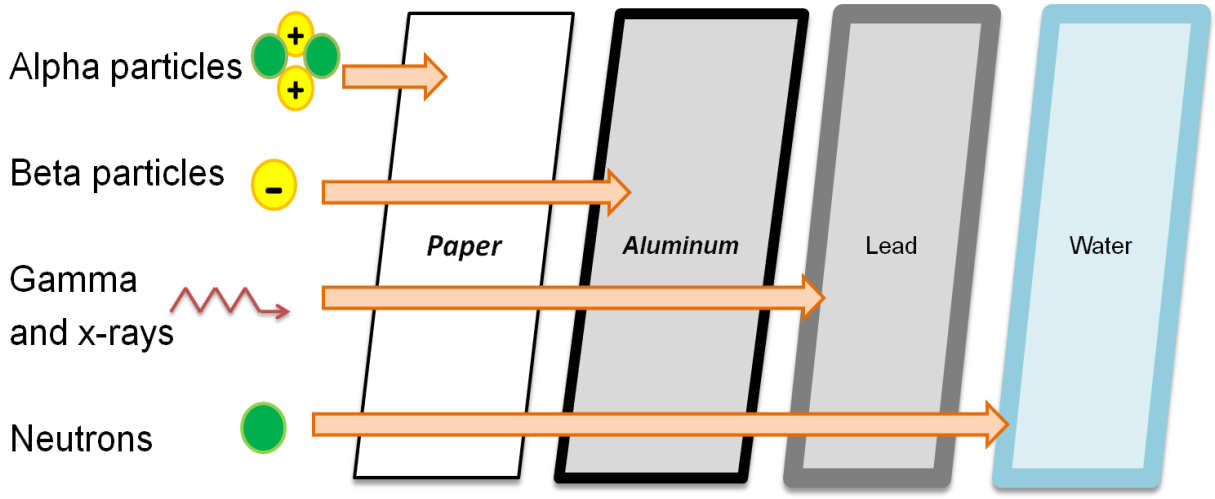

Figure 1.1 Penetrating powers of different radiation types. The yellow circles represent protons or electrons indicated with a "+" or "-" sign, respectively. The green circles are the neutrons that are uncharged particles. The red zig-zag line denotes the wave/particle nature of gamma and x-rays.

These four radiation types differ in the kind, energy and/or charge of the particle emitted and in their penetrating powers. Alpha particles are identical to a helium nucleus and usually consist of two protons and two neutrons. Beta particles are negatively charged electrons. Gamma rays and X-rays are photons which are discrete bundles of energy that exhibit both wave- and particle-like properties. Neutrons are highly energetic, uncharged particles that are highly penetrating and can cause severe DNA damage.

Exposure to IR can occur naturally, e.g. from radon decay that produces alpha particles, and cosmic rays which are high-energy radiations originating from outside the solar system. Man made sources of IR exposure occur from diagnostic procedures such as CT scans, PET scans, X-rays, radiotherapy, radiation incidents and occupational exposures. Radiation can either interact with cells directly causing damage to the DNA double helix or indirectly by interacting with water molecules that surround the DNA and producing free radicals leading to oxidative damage and hence damaging the DNA.

Chapters 2, 3 and 4 of this Dissertation present important findings on biological effects of radiation in human cells. This research provides a fundamental contribution to the field of radiation biology because it adds to our current knowledge about neutron radiation and effects of low-doses of gamma rays in human cells.

Neutrons

Neutrons are highly energetic uncharged particles that can be generated from accelerators and cyclotrons, and from decay of radioisotopes such as Californium-252.

Neutrons are the main component of cosmic radiation and are highly penetrating. The relative biological effectiveness of neutrons is between 2 to 6 compared to photons [1], meaning that 2 to 6 times less neutron dose than photon dose is needed to produce the same amount of DNA damage. The differential radiosensitivity between poorly oxygenated (more resistant) and well-oxygenated (more sensitive) cells, is reduced with neutrons. Hence, neutrons are more effective in controlling certain tumor types where conventional photon therapy is ineffective [2]. Unlike low linear energy transfer (LET) radiation (e.g. photons), for neutrons which are high-LET radiation, there is also a reduction in the differential radiosensitivity of cells related to their position in the cell cycle [3]. Patients receiving neutron or proton therapy are exposed to neutrons during treatment. In addition, astronauts, airline crews and aircraft passengers are exposed to cosmic radiation which includes neutrons. Other possible sources of neutron exposure to humans may include occupational exposure or radiation incidents such as the Hiroshima-Nagasaki atomic bomb explosions that occurred nearly 70 years ago, and the much more recent tsunami-induced radiation accident at the Fukushima Daiichi site in Japan. The radiation released from the reactors was reported to contain neutrons in addition to other radioactive particles [4].

Direct effects of neutron exposure are well known, however, not much is known about non-targeted effects (i.e. the consequences to cells neighboring the directly irradiated cells) of neutrons. Chapter 3 describes a study I performed to determine whether or not neutrons induce a bystander effect in human cells.

Bystander effect

One of the major paradigm shifts in the field of radiation biology was the discovery of the bystander effect in which cells in the vicinity of irradiated cells behave as though they were irradiated [5]. Thus, directly exposed cells are not the sole targets of radiation. The bystander effect has been observed repeatedly in mammalian cell lines in response to IR particularly consisting of photons [6-8]. Depending on the cell type, the bystander effect can be transmitted either through culture medium [9] or through cell-to-cell contact [10]. A detailed list of candidate signaling molecules that may be involved in the bystander effect is included in Chapter 3. Many studies have been performed on the radiation-induced bystander effect using photons on various cell lines, including human skin fibroblasts [11], epithelial cells [9] and leukemic cells [12, 13]. However, there is no conclusive evidence concerning a neutron-induced bystander effect in human cells.

The occurrence of the bystander effect has significant implications for risk estimation of therapeutic treatments involving radiation. Such non-targeted effects induced by radiation may have serious implications for human health and might cause cancer. Therefore, the risks of radiation exposure need to be analyzed in terms of both direct and indirect exposures.

Cytokinesis Block Micronucleus Assay (CBMN)

The CBMN assay is a well-established cytogenetic method for measuring DNA damage after exposure to radiation and other clastogens. In this assay, cells are treated with cytochalasin B to block cytokinesis leading to the formation of binucleated cells, which are first division mitotic cells that contain all the products of one mitosis inside the cell membrane. Micronuclei (MN), nuclear buds and nucleoplasmic bridges are the three different genetic endpoints that can be visualized and measured simultaneously in this assay. The major advantages of the CBMN assay are that it is reliable, simple to perform, fast, and sensitive. A single binucleated cell can have one or more of any of these three nuclear anomalies present individually or together. The molecular mechanisms behind two of the three CBMN outcomes, i.e. MN and nucleoplasmic bridges, are well known [14]. However, the mechanism of formation of nuclear buds is still unclear. MN are formed from acentric chromosomes or chromatid fragments, or when there is malsegregation of chromosomes during anaphase leading to a lagging chromosome. A single micronucleus can consist of one or more whole chromosomes and/or acentric fragments [15]. Nucleoplasmic bridges are formed when the two centromeres of a dicentric are pulled towards opposite poles during anaphase. Although the exact mechanism remains unclear, nuclear buds are thought to be formed in the process of elimination of nuclear material from the nucleus [14]. Complete details of the procedure of the CBMN assay are provided in Chapters 2 and 3. Cells can be stained either with Giemsa (Figure 1.2) or acridine orange (Figure 1.3).

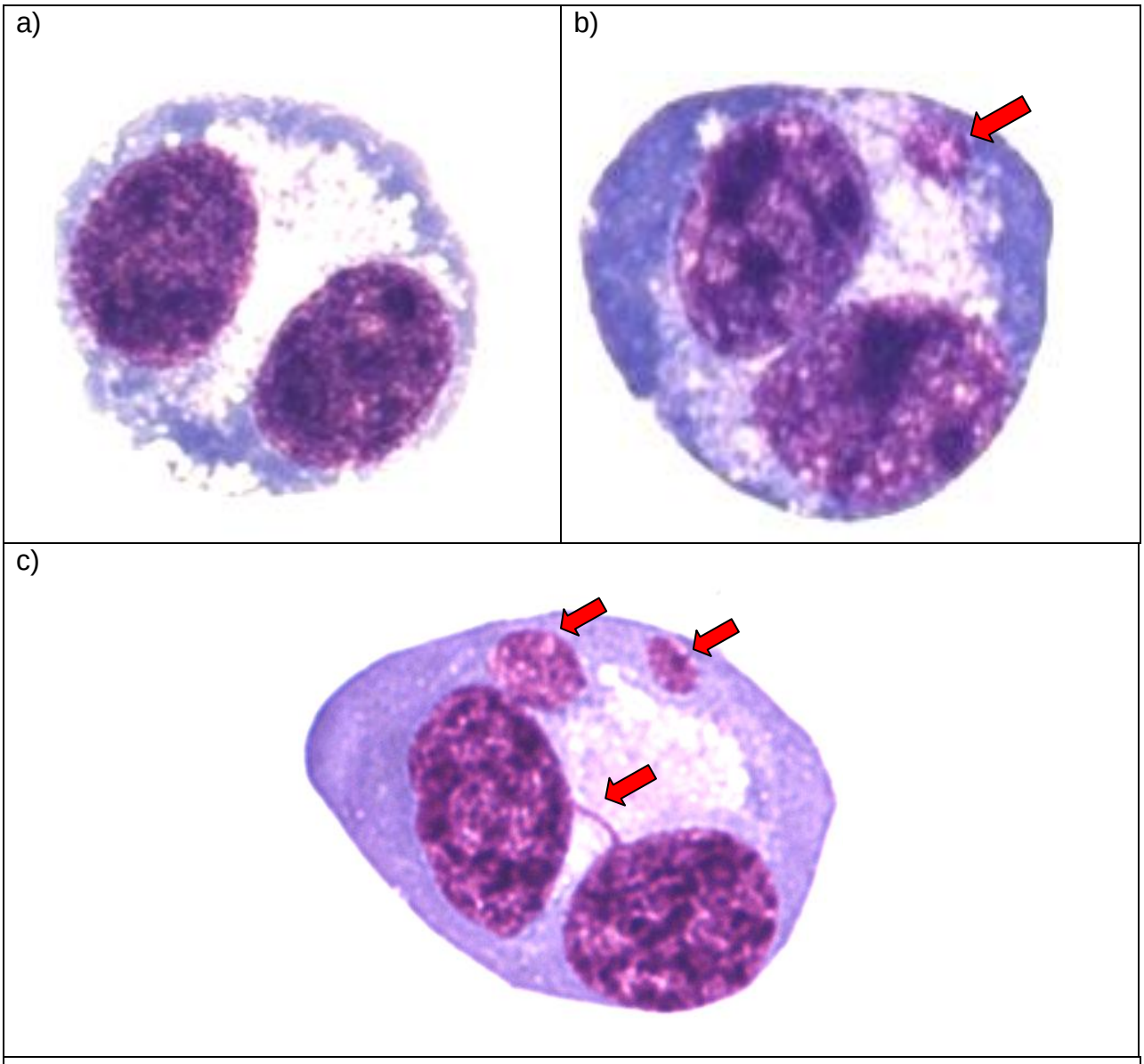

Figure 1.2 Images of binucleated cells with and without MN stained with Giemsa: a) normal binucleated cell; b) a binucleated cell with one MN; c) a binucleated cell with one MN, one nucleoplasmic bridge and a nuclear bud.

a)

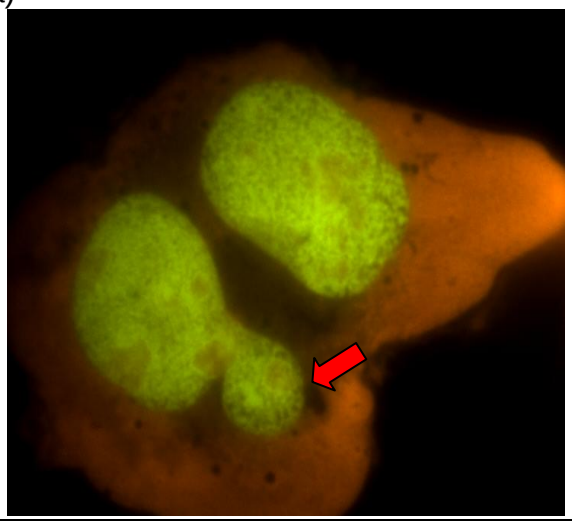

b)

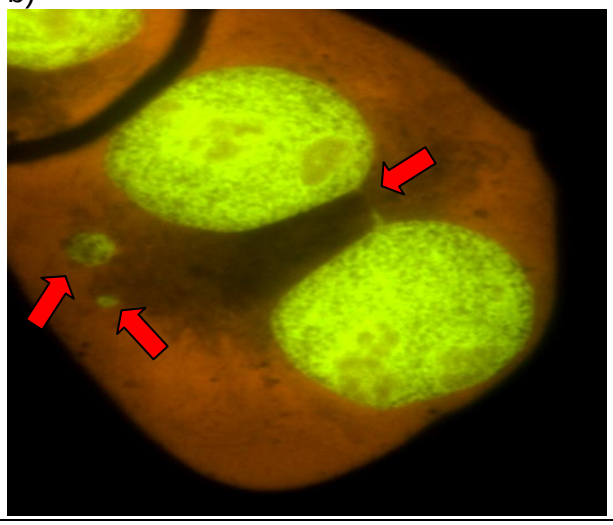

c)

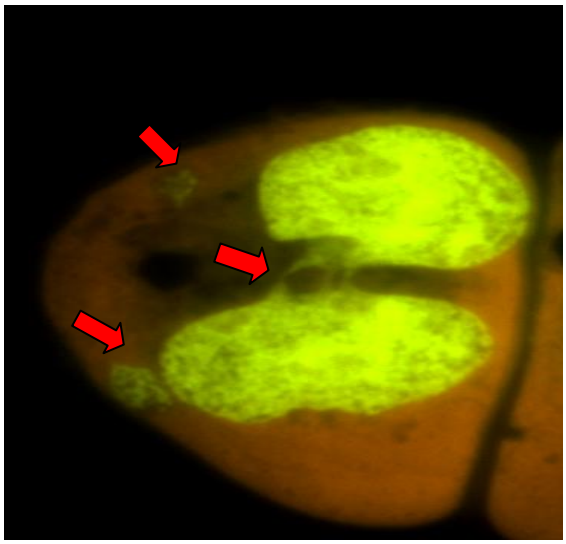

Figure 1.3 Images of binucleated cells with and without MN stained with acridine orange: a) a binucleated cell with a bud; b) a binucleated cell with two MN and one nucleoplasmic bridge; c) a binucleated cell with two MN and three bridges.

Low-dose hyper-radiosensitivity (HRS)

Some of the major effects of high doses of radiation have been known for over a century [16]. However, studies of the effects of low doses of IR have been limited by the lack of significant observable effects to the human body. One of the most important issues concerning radiation risk assessment is validation of linear-no-threshold (LNT) models. According to LNT models, the risks of genetic damage increase linearly with dose without any threshold. Due to the lack of conclusive evidence of radiation risks at very low doses, radiation protection committees assume that LNT models are true and that responses are linear at low doses [17-19]. However, phenomena such as low-dose hyper-radiosensitivity (HRS), that argue against conventional linear-no-threshold models, have been demonstrated both in vivo and in vitro in response to photons [17]. Figure 1.4 represents the different possible outcomes of the radiation dose response relationship in the very low dose region.

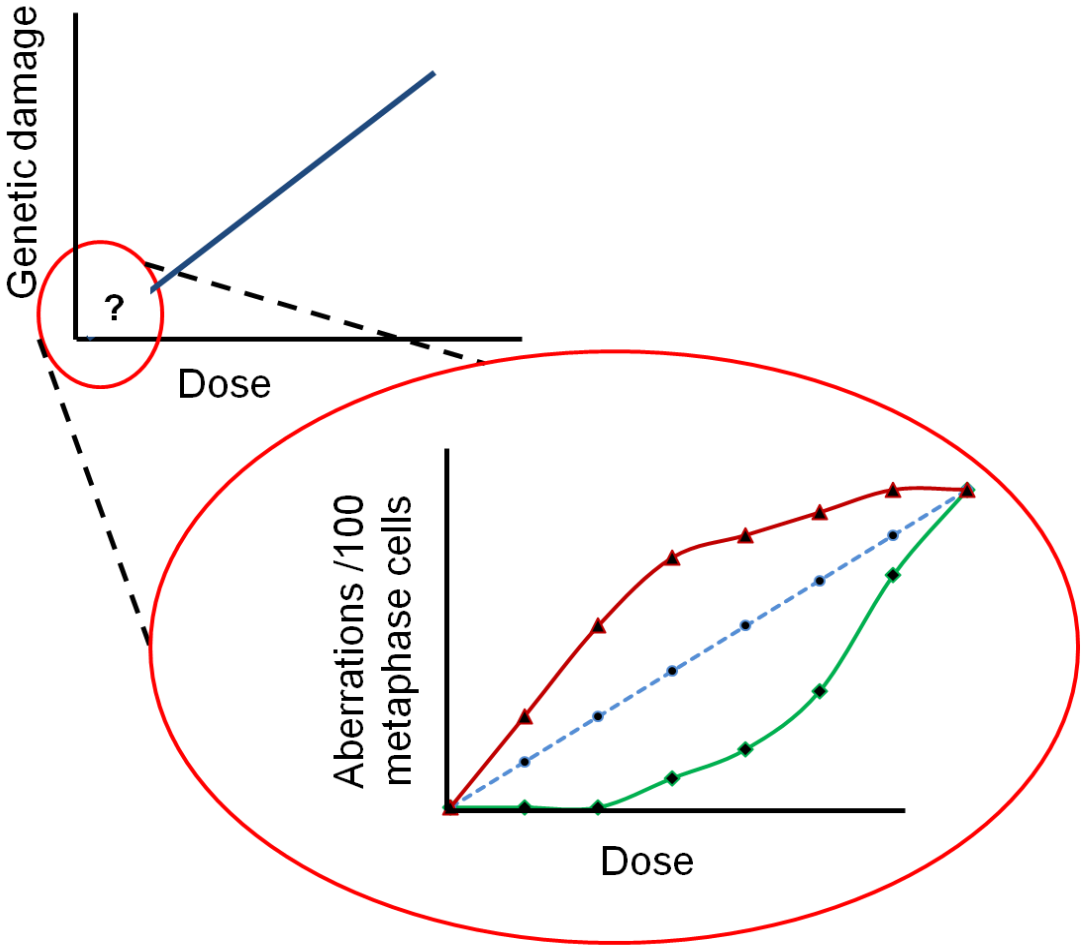

Figure 1.4 Expected outcomes of the radiation dose response relationship in the very low dose region. The diagonal line in the top graph coupled with the dotted blue line in the bottom graph represent a linear-no-threshold model that is currently followed by regulatory agencies to predict low-dose radiation risks, e.g. for cancer. The bottom graph shows two other possible outcomes of the shape of the low-dose radiation response curve for cytogenetics, where the red line depicts low-dose radiation hypersensitivity. The green line represents a threshold model where there is no damage below a certain dose.

Regulatory agencies use LNT models to extrapolate risks to low doses from high doses. The existence of HRS effects contradict LNT models and provides evidence of

non-linearity in the low dose region. In HRS, irradiated cells are at higher risk of damage per unit dose than is the case at higher doses. HRS is more prominent in the G2 phase compared to cells in the G1 or S phases of the cell cycle [19]. The existence of HRS in clonogenic survival experiments suggests that G2 phase cells with DNA damage enter mitosis due to failure of ATM-dependent DNA repair processes [18]. The damage induced by low doses of radiation is not enough to activate the DNA repair machinery. In other words, the slope of the response curve at very low doses may be significantly steeper than at higher doses. HRS may have implications in risk analysis because deviation from LNT models could necessitate a re-evaluation of radiation protection standards. The biological effects of low dose radiation and the risks associated with these effects must be considered while carrying out diagnostic and therapeutic treatments involving radiation. Chapter 4 presents the first cytogenetic evidence of low-dose hypersensitivity in human cells in response to gamma rays using structural chromosomal aberrations as the end-point.

Structural Chromosome Aberrations

One of the most sensitive yet labor intensive cytogenetic endpoints is structural chromosome aberrations. There is solid mechanistic evidence of an association of chromosomal aberrations and cancer risk, e.g. [20]. Most cancers have been associated with some form of chromosomal rearrangement (reviewed in [21]). Structural chromosomal aberration frequencies are considered to be one of the most relevant and effective biomarkers of radiation exposure [20, 22].

There are two major types of structural chromosomal aberrations: chromosome-type and chromatid-type. According to the classical theory of formation of chromosomal aberrations [23], if DNA damage occurs when the cell is in the G1 phase then that will lead to chromosome-type aberrations versus chromatid-type aberrations that are formed if DNA damage occurs in G2. Figure 1.5 demonstrates the mechanism of formation of some structural chromosomal aberration types. Translocations are well known biomarkers of exposure to radiation and are often the preferred aberration type to perform radiation dosimetry [24]. Compared to other chromosome aberrations such as dicentrics, translocations persist for significantly longer times after radiation exposure [25].

There are different methods for visualizing structural chromosomal aberrations. These include Giemsa staining of unbanded chromosomes [26] and fluorescent *in situ* hybridization (FISH) painting [27]. Giemsa stain is inexpensive but scoring Giemsa stained chromosomes can be challenging and labor intensive. FISH painting probes are very expensive but scoring these cells is comparatively easy and less labor-intensive than scoring Giemsa-stained chromosomes. FISH-painting is not needed for identifying chromatid exchanges, and may in fact interfere with their identification because painting involves denaturation of the chromosomes, which can obscure some of the more subtle changes in certain chromosomal aberrations. With Giemsa staining all kinds of chromatid-type damage (e.g. triradials and quadriradials) and much of the chromosome-type damage including dicentrics, fragments, and rings can be clearly identified. The major disadvantage of Giemsa staining is that many translocations, insertions,

deletions, and duplications cannot be identified [28]. Figure 1.6 shows pictures of Giemsa stained chromosomes in metaphase.

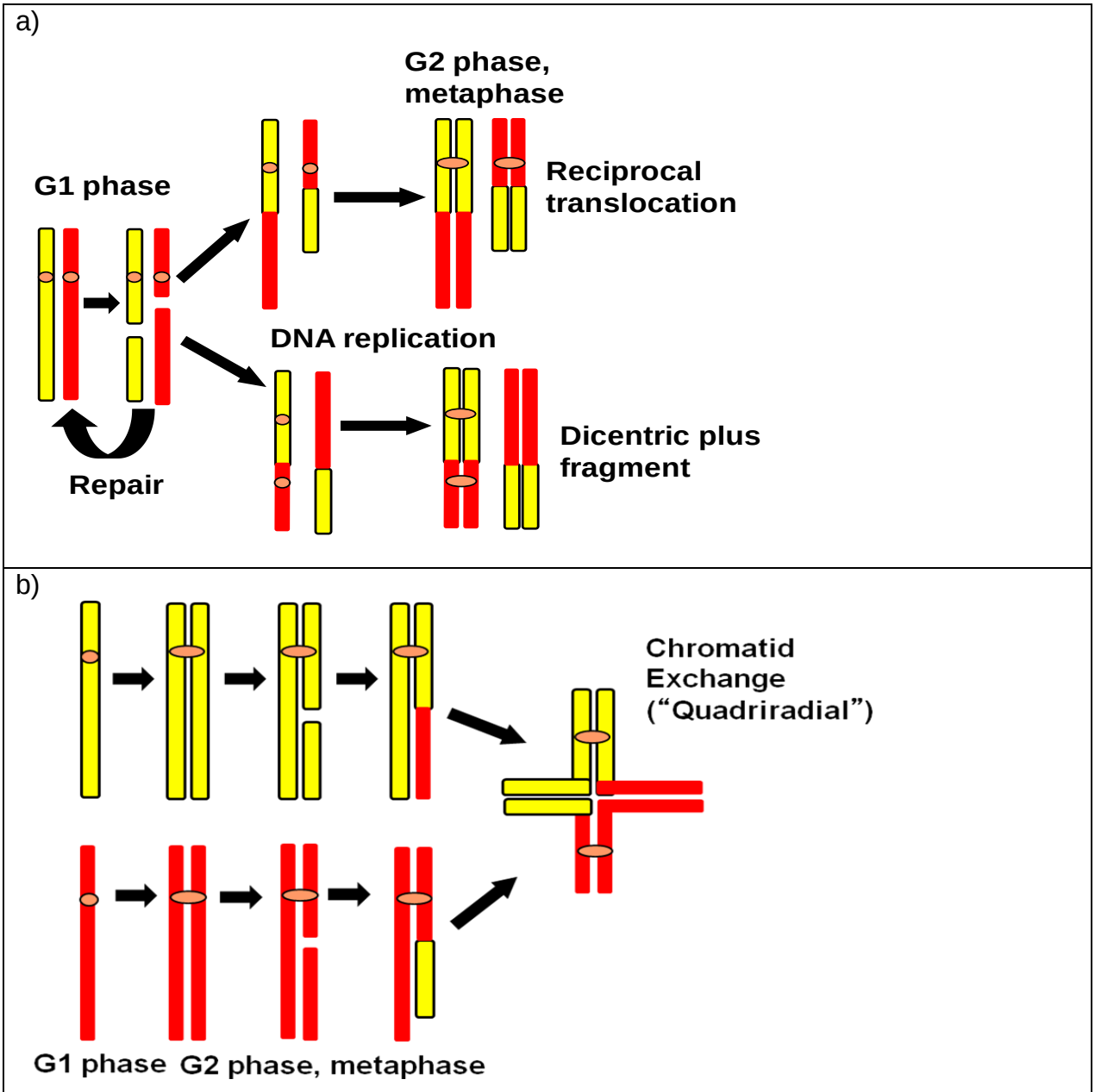

Figure 1.5 Mechanism of formation of some structural chromosomal aberrations. a) a break in each of two non-homologous chromosomes (depicted by yellow and red colors) in G1 can either lead to a stable rearrangement called a reciprocal translocation where there is an exchange of fragments or it can lead to the formation of a dicentric and an acentric fragment; b) a break in one of the chromatids in each of two chromosomes in G2 can lead to an exchange of chromatid fragments resulting in formation of a quadriradial.

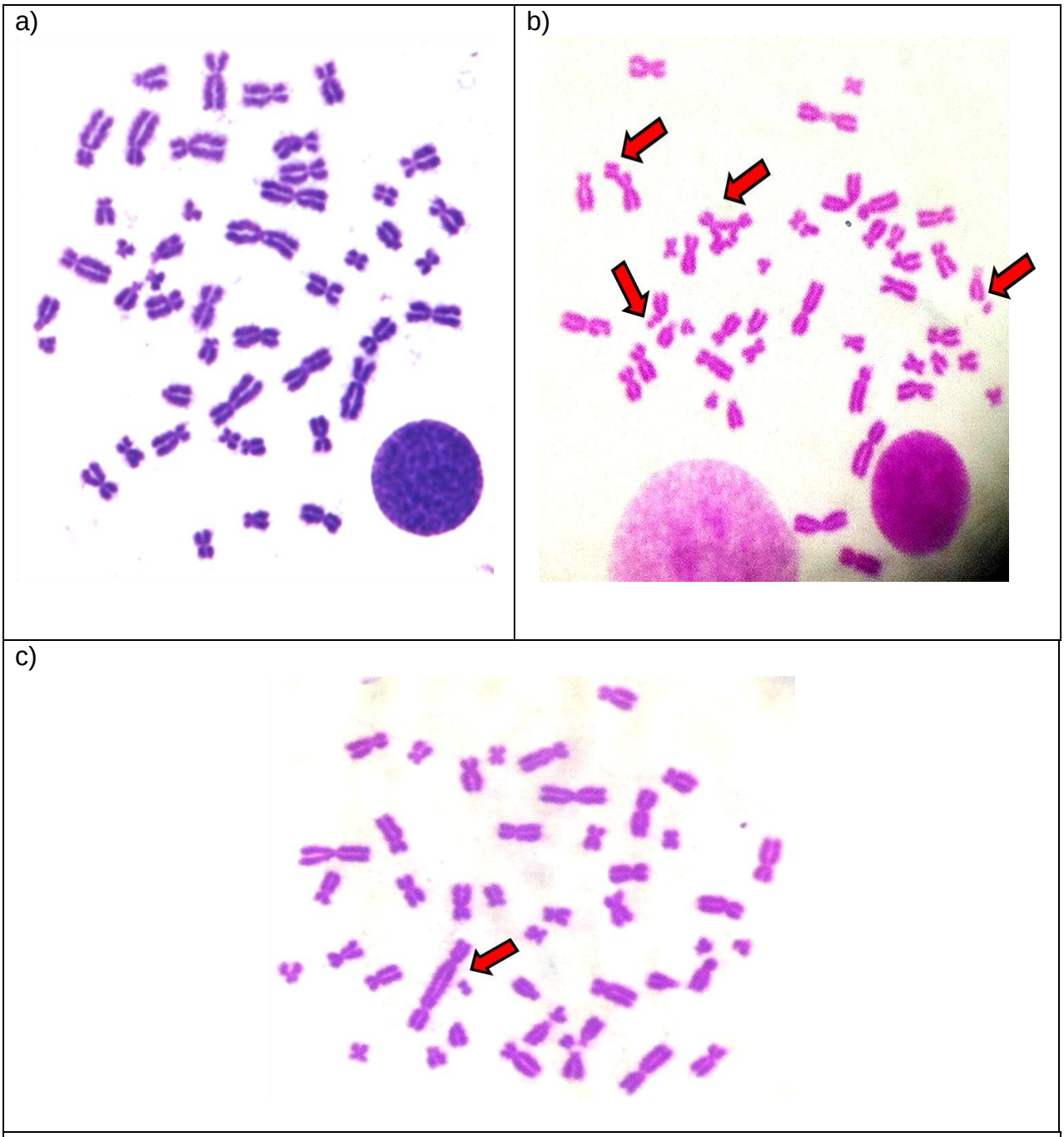

Figure 1.6 Examples of cells in metaphase stained with Giemsa showing structural chromosomal aberrations: a) normal human cell in metaphase stained with Giemsa; b) cell with an asymmetrical chromatid exchange ("quadriradial") and chromatid breaks (arrows); and c) cell with a dicentric and a fragment next to it (arrow).

Future Directions

Neutrons and the bystander effect

Chapter 3 answers an important question regarding whether neutrons induce a bystander effect in human cells. Even though neutron therapy has the potential to treat tumors that cannot be treated as effectively by photon radiotherapy or chemotherapy, no conclusive evidence exists to support or refute the existence of non-targeted effects of neutrons in human cells. Information obtained from this study will facilitate refined estimates of the risk-benefit ratio of neutron therapy and may be valuable to those who are concerned about the health effects of exposure during space travel. Understanding the biological effects of neutrons may also enable more refined evaluations of the standards for radiation protection and safety.

Characterization of the radiation response curve at low doses

Chapter 4 provides cytogenetic evidence of low-dose hyper-radiosensitivity in the G2 phase in human peripheral blood lymphocytes. This is the first time that the shape of the radiation dose response curve in G2 has been characterized at such low doses using structural chromosomal aberrations. Determining the shape of the low-dose response may lead to improvements in the evaluation of radiation risks. Low-dose radiation hypersensitivity could be exploited clinically if radiotherapy were delivered in a large number of dose fractions, each of which is less than 0.5 Gy. The net effect of low-dose hypersensitivity on cancer risks in cell populations and tissues will depend on whether the increased damage occurring at these low doses results in increased

cytotoxicity and/or more survivable mutations. Further work needs to be done to couple mutational assays with the ultimate fate of cells after damage by low doses of radiation.

REFERENCES

1. Seth, I., et al., *Neutron exposures in human cells: bystander effect and relative biological effectiveness.* PLoS One, 2014. **9**(6): p. e98947.
2. Lennox, A.J., *High-Energy Neutron Therapy for Radioresistant Cancers*, in *International Conference on Advanced Neutron Sources – XVIII*. Dongguan, Guangdong, China.
3. Joiner, M.C. and A. Van_der_Kogel, *Basic Clinical Radiobiology*. 4th ed. 2009, London, UK: Macmillan Publishing Solutions.
4. Priyadarshi, A., G. Dominguez, and M.H. Thiemens, *Evidence of neutron leakage at the Fukushima nuclear plant from measurements of radioactive 35S in California.* Proc Natl Acad Sci U S A, 2011. **108**(35): p. 14422-5.
5. Mothersill, C. and C. Seymour, *Radiation-induced bystander effects, carcinogenesis and models.* Oncogene, 2003. **22**(45): p. 7028-33.
6. Asur, R.S., R.A. Thomas, and J.D. Tucker, *Chemical induction of the bystander effect in normal human lymphoblastoid cells.* Mutat Res, 2009. **676**(1-2): p. 11-6.
7. Maguire, P., et al., *Medium from irradiated cells induces dose-dependent mitochondrial changes and BCL2 responses in unirradiated human keratinocytes.* Radiat Res, 2005. **163**(4): p. 384-90.
8. Rajendran, S., et al., *The role of mitochondria in the radiation-induced bystander effect in human lymphoblastoid cells.* Radiat Res, 2011. **175**(2): p. 159-71.
9. Mothersill, C. and C. Seymour, *Medium from irradiated human epithelial cells but not human fibroblasts reduces the clonogenic survival of unirradiated cells.* Int J Radiat Biol, 1997. **71**(4): p. 421-7.

10. Edwards, G.O., et al., *Gap junction communication dynamics and bystander effects from ultrasoft X-rays.* Br J Cancer, 2004. **90**(7): p. 1450-6.

11. Mothersill, C. and C. Seymour, *Radiation-induced bystander effects and adaptive responses--the Yin and Yang of low dose radiobiology?* Mutat Res, 2004. **568**(1): p. 121-8.

12. Konopacka, M. and J. Rzeszowska-Wolny, *The bystander effect-induced formation of micronucleated cells is inhibited by antioxidants, but the parallel induction of apoptosis and loss of viability are not affected.* Mutat Res, 2006. **593**(1-2): p. 32-8.

13. Mitra, A.K. and M. Krishna, *Radiation-induced bystander effect: activation of signaling molecules in K562 erythroleukemia cells.* J Cell Biochem, 2007. **100**(4): p. 991-7.

14. Fenech, M., et al., *Molecular mechanisms of micronucleus, nucleoplasmic bridge and nuclear bud formation in mammalian and human cells.* Mutagenesis, 2011. **26**(1): p. 125-32.

15. Eastmond, D.A. and J.D. Tucker, *Identification of aneuploidy-inducing agents using cytokinesis-blocked human lymphocytes and an antikinetochore antibody.* Environ Mol Mutagen, 1989. **13**(1): p. 34-43.

16. Upton, A.C., *The first hundred years of radiation research: what have they taught us?* Environ Res, 1992. **59**(1): p. 36-48.

17. Joiner, M.C., et al., *Low-dose hypersensitivity: current status and possible mechanisms.* Int J Radiat Oncol Biol Phys, 2001. **49**(2): p. 379-89.

18. Krueger, S.A., et al., *Role of apoptosis in low-dose hyper-radiosensitivity.* Radiat Res, 2007. **167**(3): p. 260-7.

19. Marples, B., B.G. Wouters, and M.C. Joiner, *An association between the radiation-induced arrest of G2-phase cells and low-dose hyper-radiosensitivity: a plausible underlying mechanism?* Radiat Res, 2003. **160**(1): p. 38-45.

20. Bonassi, S., et al., *Chromosomal aberration frequency in lymphocytes predicts the risk of cancer: results from a pooled cohort study of 22 358 subjects in 11 countries.* Carcinogenesis, 2008. **29**(6): p. 1178-83.

21. Frohling, S. and H. Dohner, *Chromosomal abnormalities in cancer.* N Engl J Med, 2008. **359**(7): p. 722-34.

22. Bonassi, S., et al., *Chromosomal aberrations and risk of cancer in humans: an epidemiologic perspective.* Cytogenet Genome Res, 2004. **104**(1-4): p. 376-82.

23. Savage, J.R., *Classification and relationships of induced chromosomal structual changes.* J Med Genet, 1976. **13**(2): p. 103-22.

24. Tucker, J.D., *Low-dose ionizing radiation and chromosome translocations: a review of the major considerations for human biological dosimetry.* Mutat Res, 2008. **659**(3): p. 211-20.

25. Tucker, J.D., *Chromosome translocations and assessing human exposure to adverse environmental agents.* Environ Mol Mutagen, 2010. **51**(8-9): p. 815-24.

26. Mateuca, R., et al., *Chromosomal changes: induction, detection methods and applicability in human biomonitoring.* Biochimie, 2006. **88**(11): p. 1515-31.

27. Tucker, J.D., D.A. Lee, and D.H. Moore, 2nd, *Validation of chromosome painting. II. A detailed analysis of aberrations following high doses of ionizing radiation in vitro.* Int J Radiat Biol, 1995. **67**(1): p. 19-28.

28. Bayani, J. and J.A. Squire, *Traditional banding of chromosomes for cytogenetic analysis.* Curr Protoc Cell Biol, 2004. **Chapter 22**: p. Unit 22 3.

CHAPTER 2

This chapter has been previously published in the journal “Mutagenesis”. I am a joint first-author on this paper. In this chapter I have only included data from this paper that are from experiments I performed myself. The citation of this paper is:

Cheong HS, Seth I, Joiner MC, Tucker JD., 2013. Relationships among micronuclei, nucleoplasmic bridges and nuclear buds within individual cells in the cytokinesis-block micronucleus assay. Mutagenesis 28:433-440.

Relationships among micronuclei, nucleoplasmic bridges and nuclear buds within individual cells in the cytokinesis-block micronucleus assay

INTRODUCTION

Cytogenetic analyses have been used to answer many questions concerning the effects of ionizing radiation and potentially clastogenic chemicals in a wide variety of organisms. The cytokinesis-block micronucleus (CBMN) assay is a well-established method that can be used to measure DNA damage in human lymphocytes [1]. This assay involves the application of cytochalasin B, an inhibitor of actin polymerization, to block cytokinesis in mitotic cells. Cells undergoing a single round of mitosis thus become binucleated and are easily distinguished from undivided cells. The CBMN assay is a multi-endpoint method that can be used to measure different biomarkers of DNA damage. The three different end points that can be analyzed simultaneously in this assay are micronuclei, nucleoplasmic bridges and nuclear buds.

Until recently, most studies involving the CBMN assay have considered only micronucleus frequencies and have not evaluated bridges or buds. Micronucleus frequencies are not always simple to interpret because micronuclei may originate by many mechanisms. The action of clastogens gives rise to micronuclei that contain mainly acentric chromosome or chromatid fragments, and these can occur through DNA double-strand breaks (DSBs), or single-strand breaks that are converted into DSBs after DNA replication, or inhibition of DNA synthesis [2]. Micronuclei may also result from lagging whole chromosomes in mitosis due to spindle attachment errors, defects in centromeres and/or kinetochores or abnormal cell cycle check points [2]. Furthermore, micronuclei may be generated by elimination of double minutes by nuclear budding or lagging of double minutes in mitosis [3]. The fragmentation of nucleoplasmic bridges has also been observed to result in the formation of micronuclei [4]. Several modifications that have been made to the assay enable determination of the origins of the induced micronuclei; e.g. the effects of aneugenic or clastogenic agents can be identified using centromere-specific DNA probes or anti-kinetochore antibodies [5-7].

Nucleoplasmic bridges are another indicator of DNA damage and are easily observable alongside micronuclei in the CBMN assay, requiring no additional sample preparation. Bridges originate from dicentric chromosomes which are formed through misrepair of DNA breaks and telomere fusion events [8, 9]. Due to these highly specific origins, scoring of bridges may aid in the interpretation of micronucleus data or provide additional information that is not available through the scoring of micronuclei alone. Previous work has also shown that both micronuclei and bridge induction occur in response to ionizing radiation and reactive oxygen species, and that these increases

are highly correlated [10]. In addition, high correlations between these three genetic end points have been shown in response to folic acid deficiency [11, 12].

Nuclear buds may also be observed with the CBMN assay. Buds have been shown to form by the elimination of amplified extrachromosomal DNA during interphase as an intermediate step in the formation of double minute-type micronuclei [3, 13], and also occur from the remnants of broken nucleoplasmic bridges [14]. A correlated increase in micronuclei and buds has been demonstrated in cells treated with mitomycin C or Colcemid® [15].

Many improvements in the CBMN assay have been made since it was first described [16]. Although studies evaluating the effects of many DNA damaging agents including ionizing radiation and chemicals such as mitomycin C [17] and phleomycin [18] have been performed using this assay, there are no published data describing the statistical associations among micronuclei, bridges and buds within each cell. These three end points are important because of the different mechanisms by which each arises. This might yield insights into the different kinds of damage to cells. In the current study, cells treated with gamma radiation and neutron radiation were analyzed. Here we report that the presence of any one of these three genetic end points in a given cell is significantly associated with an increased probability for the presence of the remaining two outcomes.

MATERIALS AND METHODS

Cell lines

Two normal human lymphoblastoid cell lines, GM15510 and GM15036, were obtained from the Coriell Cell Repository.

Cell culture techniques

Cells were cultured according to the standard protocol provided by Coriell. Cells were grown in T25 or T75 CellStar vented suspension culture flasks (Greiner Bio-one) containing RPMI-1640 medium (Thermo Scientific) that was supplemented with 15% fetal bovine serum (Atlanta Biological). In addition, penicillin-streptomycin (100 U/mL penicillin, 100 µg/mL streptomycin) (Gibco), 2 mM L-glutamine (Gibco), and 2.5 µg/mL amphotericin B (Thermo Scientific) were added to the medium. The volumes of culture did not exceed 20 mL for T25 flasks or 60 mL for T75 flasks. Cell culture flasks were kept in a fully humidified incubator at a temperature of 37°C and CO_2 concentration of 5%. Cells were seeded at 3×10^5 cells/mL and passaged when the concentration reached approximately 1×10^6 cells/mL (3-6 days from time of previous passage depending on the cell line). Cells were fed at intervals of 3 days after passage by careful removal of approximately half of the culture medium in flasks without disturbing sedimented cells, and addition of the same volume of fresh cell culture medium. All cell culture media were pre-warmed to 37°C before use.

Experimental design for gamma radiation and neutron radiation

Cells were seeded at 3.0×10^5 cells/mL in 10 mL of culture medium in T25 non-vented flasks (Greiner Bio-one) and incubated overnight with loosened caps. All irradiations were performed in the Gershenson Radiation Oncology Center, Wayne State University, Detroit, Michigan. For neutron exposures the cells were cultured in T25 flasks but immediately prior to irradiation the cells were transferred to polypropylene Falcon tubes (Evergreen Scientific, Los Angeles, CA). A cyclotron was used to generate d(48.5)-Be neutrons with the dose rate of 0.3 Gy/min at doses of 0 (control), 0.5, 1, 1.5, 2, 3 and 4 Gy. Following exposure the cells were returned immediately to the laboratory, transferred to new T25 culture flasks, and incubated as described. For the neutron radiations given with this clinical machine, six percent of the total dose (neutrons plus gamma rays) is due to contamination from γ-radiation produced mostly by the absorption of neutrons in the beam collimator, as is always the case with particle irradiators. For evaluation of damage induced by low-dose γ-radiation only, cultures of GM15510 and GM15036 were acutely irradiated with a Cobalt-60 source using a Theratron radiotherapy unit (Atomic Energy of Canada), with the dose rate of 0.25 Gy/min. The doses used were equivalent to the six percent contamination of γ-radiation in the neutron beam exposures, i.e. 0 (control), 0.03, 0.06, 0.09, 0.12, 0.18 and 0.24 Gy. To evaluate effects of higher doses of γ-radiation, cells were also irradiated in a separate experiment with γ-radiation doses of 0 (control), 0.5, 1, 2, 3 and 4 Gy. For γ-radiation, cells were cultured in T25 flasks and irradiated, after which they were brought back to the laboratory and returned to the incubator for four hours.

Cytokinesis-block micronucleus assay

Following four hours of incubation, 6 µg/ml of cytochalasin B (Sigma) was added to each culture. A stock of 600 µg/mL cytochalasin B in dimethyl sulfoxide was used, for a final dimethyl sulfoxide concentration of 1% in treated cultures. Twenty eight hours after addition of cytochalasin B, cells were harvested by centrifugation onto ethanol-cleaned glass slides using a StatSpin Cytofuge 2 cytocentrifuge. After drying briefly in air, the cells were fixed in 100% methanol for 15 minutes.

Giemsa staining and slide preparation

Fixed slides were immersed in 5% Giemsa, prepared by diluting 2.5 mL Giemsa stain (Acros Organics) in 47.5 mL dH_2O, for 20 minutes. Slides were then rinsed briefly in dH_2O and air-dried. For long-term storage, slides were mounted with a drop of Permount (Fisher Scientific) and 22x22 mm^2 or 25x25 mm^2 glass coverslips.

Data collection

All slides were read by trained scorers on Nikon Eclipse E200 light microscopes at 1000× magnification, and were coded prior to scoring to prevent observer bias. For 0.5 Gy to 4 Gy γ-irradiated slides, approximately 500 cells were scored by each of two trained people for a total of approximately 1000 binucleated cells per treatment group.

For cell lines treated with neutron radiation or low-dose γ-radiation (0.03 Gy to 0.24 Gy), 1,200 to 18,000 binucleated cells were scored for each treatment condition. A large number of cells had to be scored for low doses of γ-radiation because these doses induce low levels of damage for each of the three biomarkers. The scoring was performed by trained observers and was balanced between 2 to 4 scorers such that for each dose, each scorer evaluated approximately the same number of cells.

To determine whether there were enough binucleated cells for each treatment condition, the mean number of nuclei per cell was determined by counting 300 to 400 cells. These data indicated that the numbers of binucleated cells were high enough to enumerate micronuclei, bridges, and buds for every treatment condition except for cells irradiated with 3 or 4 Gy neutrons. For low doses of photons, determination of the mean number of nuclei was not necessary because doses higher than these had enough binucleated cells to enumerate all three end points.

Cell scoring criteria

Cells were scored essentially according to established criteria [19, 20], with refinements as illustrated in Figure 2.1. For the neutron experiments, all binucleated cells with non-overlapping nuclei were included for evaluation; this includes cells where the two nuclei were touching each other, as shown in Figure 2.1b and 2.1c. This approach is referred to here as the “relaxed” criteria. For the γ-radiation experiments, the nuclei were required to be well-separated and not in contact with each other at any point, as shown in Figure 2.1d. This approach is referred to here as the “stringent”

criteria. For all experiments the cells were also required to have fully intact cytoplasm with boundaries that were clearly distinct from adjacent cells. All cells were evaluated simultaneously for three different end points: micronuclei, bridges, and buds, and the coincident presence of these endpoints within individual cells were recorded. Entities were considered to be micronuclei if they had similar color and texture to the main nuclei, had a diameter of less than one-third that of the main nuclei, were round or oval with a clear and well-defined boundary, and were located fully within the cytoplasm. Nucleoplasmic bridges were considered to be fully continuous extensions of nucleoplasm that spanned from one nucleus to the other, with similar staining characteristics to nuclei. Nuclear buds were required to appear similar to micronuclei and had to be visibly attached to a single main nucleus via a stalk that was narrower than the widest point across the bud.

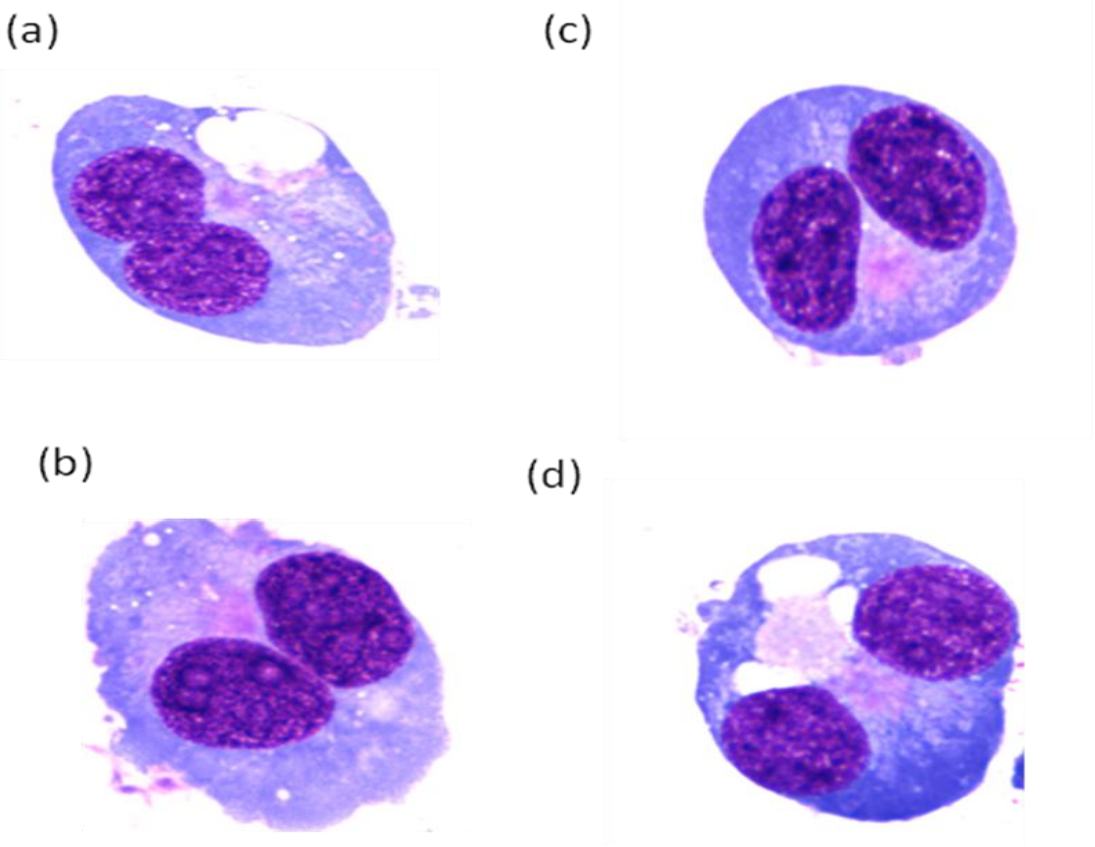

Figure 2.1 Human binucleated lymphoblastoid cells showing (a) overlapping nuclei, (b, c) touching nuclei, and (d) well-separated nuclei. The cells in (b), (c), and (d) were counted when using the relaxed criteria for the CBMN assay, while only cells of the type shown in (d) were counted using the stringent criteria which enabled observation of the nucleoplasmic bridges.

Statistical analyses

The odds ratios for the presence of micronuclei, bridges and buds in cells were calculated for each radiation dose for each cell line within each treatment condition. Homogeneity of the odds ratios within the treatment sets were evaluated by Woolf's test of heterogeneity [21]. If no significant heterogeneity of the odds ratios was found, the

hypotheses that the common odds ratios for each cell line within each treatment group were greater than 1 was evaluated by the Mantel-Haenszel Chi-square test with continuity correction [22]. All statistical analyses were performed using R version 2.15.0 with the vcd package version 1.2-13.

RESULTS AND DISCUSSION

All treatment of cell lines with γ-radiation or neutron radiation induced a radiation dose-dependent increase in micronuclei, bridges and buds (Figure 2.2).

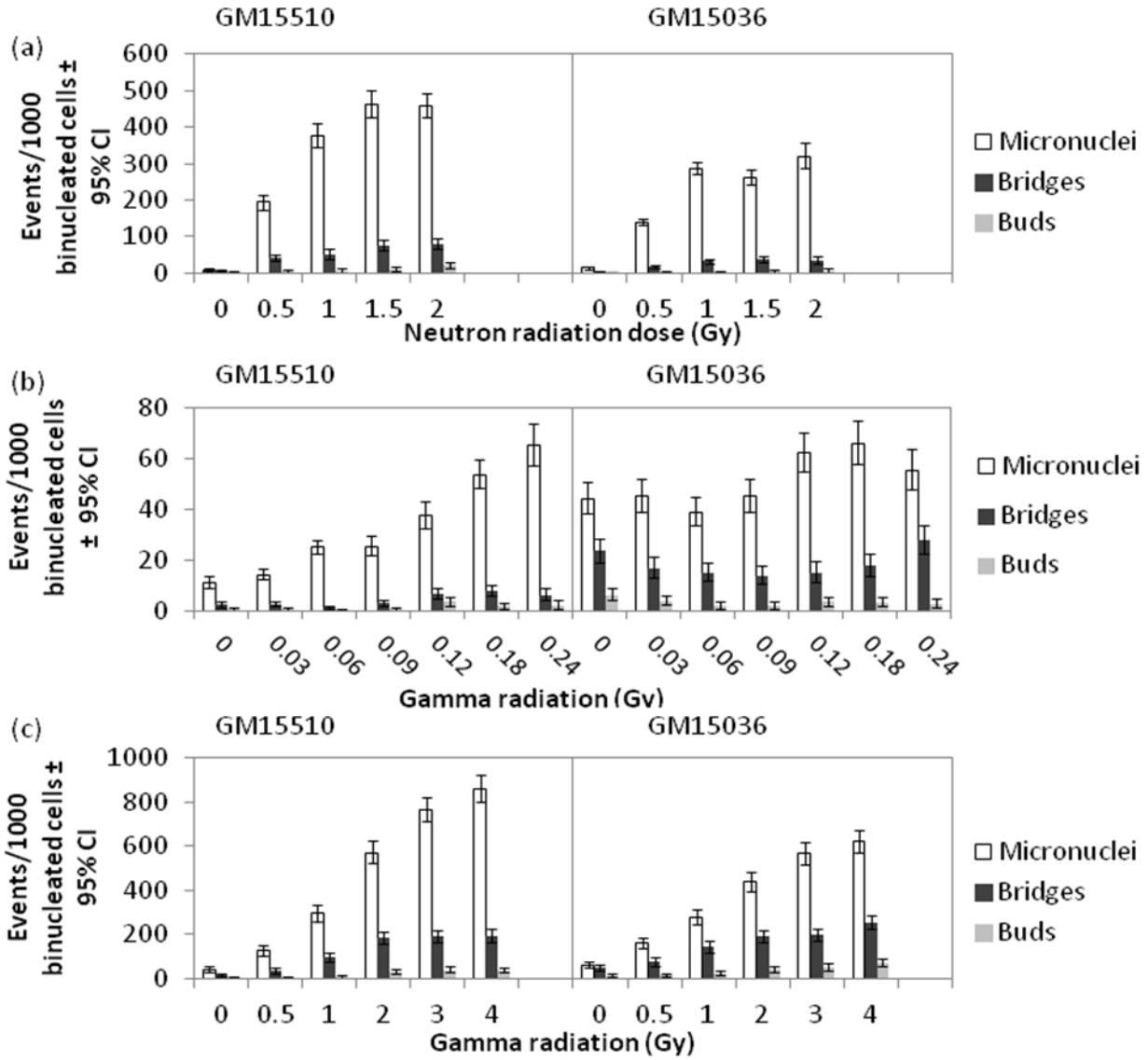

Figure 2.2 Induction of micronuclei, nucleoplasmic bridges and nuclear buds evaluated with the CBMN assay in two normal human lymphoblastoid cell lines irradiated with (a) neutrons, (b) low doses of Cobalt-60 γ-radiation and (c) high doses of Cobalt-60 γ-radiation. Cells scored in (a) and (b) were evaluated using the relaxed criteria, while cells in (c) were evaluated with the stringent criteria as described in the Materials and Methods section.

All cell lines showed decreases in the average number of nuclei per cell with increasing radiation dose, consistent with increasing cytotoxicity of the treatments with dose (Tables 2.1 and 2.2). The dose responses shown by these data are in general agreement with prior work from our laboratory [18, 23].

Table 2.1. Average number of nuclei per cell for cultures treated with Cobalt-60 γ-radiation.

γ-radiation dose (Gy)	Nuclear division index	
	GM15510	GM15036
0	1.61	1.33
0.5	1.54	1.28
1	1.50	1.25
2	1.14	1.18
3	1.08	1.10
4	1.05	1.15

Table 2.2. Average number of nuclei per cell for cultures treated with neutrons.

Neutron radiation dose (Gy)	Nuclear division index	
	GM15510	GM15036
0	1.73	2.01
0.5	1.50	1.65
1	1.37	1.42
1.5	1.11	1.21
2	1.21	1.12
3	1.08*	1.05*
4	1.09*	1.06*

*indicates too few binucleated cells to score for micronuclei, bridges, and buds.

Two different approaches to scoring binucleated cells were used in this study; these differed with respect to the physical distance that was required to exist between the two nuclei in each cell being considered for analysis. The “stringent” scoring criteria required the nuclei to have substantial distance between them, while the “relaxed” scoring criteria allowed the nuclei to be touching, as shown in Figure 2.1. Only the scoring itself differed between each set of criteria; slides were otherwise prepared with identical materials and procedures, and criteria for determining whether an entity within the cytoplasm was to be considered a micronucleus, bridge or bud were unchanged. To evaluate the effects of increasing the stringency of scoring criteria on counts of micronuclei, bridges and buds, a single observer scored eleven slides of γ-irradiated (0, 0.5, 1, 2, 3 and 4 Gy) normal human lymphoblastoid cells. Each of these slides was evaluated first with the relaxed criteria and subsequently with the stringent criteria. A direct comparison of the results produced by these two scoring methods showed that while micronuclei and bud frequencies did not differ substantially between the two criteria, the frequency of bridges was two-fold higher when evaluated with the stringent criteria compared to the relaxed criteria (data not shown). This higher value may better represent the true frequency of bridges in these samples. However, it should be noted that use of the stringent criteria also resulted in nearly a seventy percent reduction in the number of scoreable cells obtained from each slide. This comparison of scoring methods suggests that the use of stringent criteria aids significantly in the observation of bridges compared to the relaxed criteria, with the caveat of an almost three-fold reduction in the number of scoreable cells. Two strategies that may be used in the future to help overcome this large loss of scoreable cells are to increase the number of

cells per slide and to increase the proportion of scoreable cells. The first may be achieved by using a higher concentration of cells when spinning them onto slides. The second may be carried out by increasing the centrifugation speed and perhaps by hypotonic pre-treatment of cells.

Cells treated with either γ-radiation or neutron radiation were then evaluated using either the stringent or the relaxed criteria, with cell counts ranging from 1000 to 18,000 binucleated cells depending on the treatment condition, with lower doses generally having more cells counted. Three different cytogenetic endpoints, i.e. micronuclei, nucleoplasmic bridges, and buds, were evaluated simultaneously in each cell, regardless of the scoring criterion employed, and the number of cells with at least one of these endpoints present ranged from a low of 45 in control treatments to a high of 1078 in irradiated cultures. For each treatment condition, all the common odds ratios for the presence of micronuclei and nucleoplasmic bridges were found to be significantly higher than 1.00 (Table 2.3), indicating that the presence of bridges is a significant risk factor for the presence of micronuclei within a cell, and vice versa.

Table 2.3. Common odds ratios for the associations between MN and bridges, MN and buds, and buds and bridges.

Associated events	Treatment	Common odds ratio estimates	
		GM15510	GM15036
MN and Bridges	Neutron radiation	7.71	4.79
	γ-radiation (low doses)	15.38	5.33
	γ-radiation (high doses)	6.69	4.96
MN and Buds	Neutron radiation	2.69	2.64
	γ-radiation (low doses)	5.39	6.88
	γ-radiation (high doses)	—†	1.50
Buds and Bridges	Neutron radiation	4.43	4.57
	γ-radiation (low doses)	5.55	6.94
	γ-radiation (high doses)	2.34	—†

† Common odds ratio could not estimated due to significant heterogeneity ($p < 0.05$) in the odds ratios

Additionally, within each cell line, the odds ratios for the presence of micronuclei and bridges for each treatment condition do not differ significantly from each other (Figure 2.3a, 2.4a and 2.5a), indicating that the effects of the presence of bridges on the presence of micronuclei (and vice versa) are fairly constant despite changes in radiation doses. In addition, between the two normal human lymphoblastoid cell lines, the common odds ratios for micronuclei and bridges for both types of radiation are similar. This suggests that regardless of the genotype, the mechanism for the formation of micronuclei and bridges remains the same in different cell lines and for different types of

radiation. These relationships were consistent across both the stringent and the relaxed scoring criteria despite the differences in the frequencies of bridges as already shown.

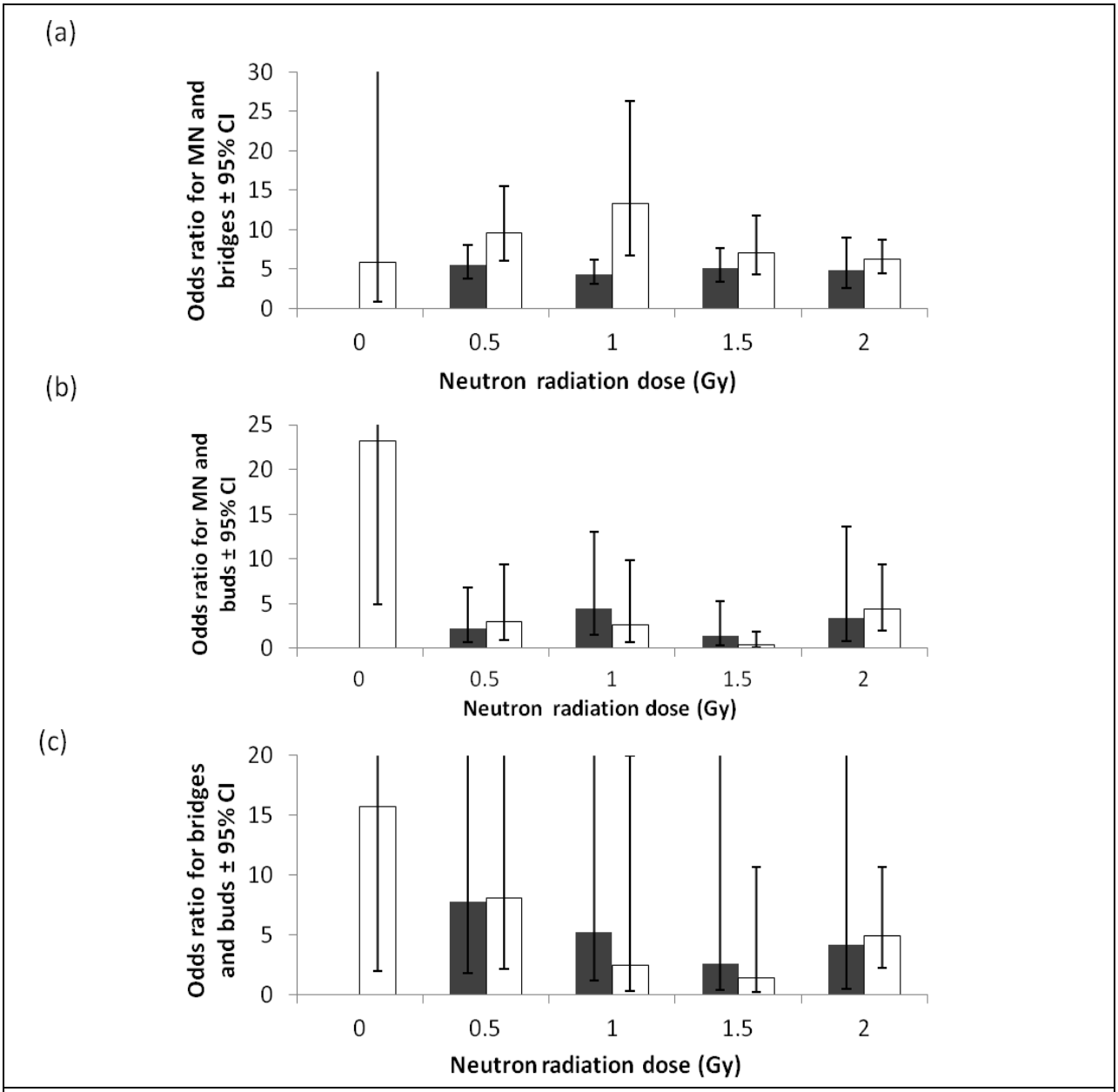

Figure 2.3 Odds ratios for the simultaneous presence (a) of micronuclei (MN) and nucleoplasmic bridges, (b) micronuclei and buds, and (c) bridges and buds in two normal human lymphoblastoid cell lines treated with neutrons. Some upper confidence intervals have been truncated to provide a closer look at the data. Missing values at the 0-doses indicate that the odds ratio could not be calculated due to a lack of cells containing one or both of the two endpoints being evaluated.

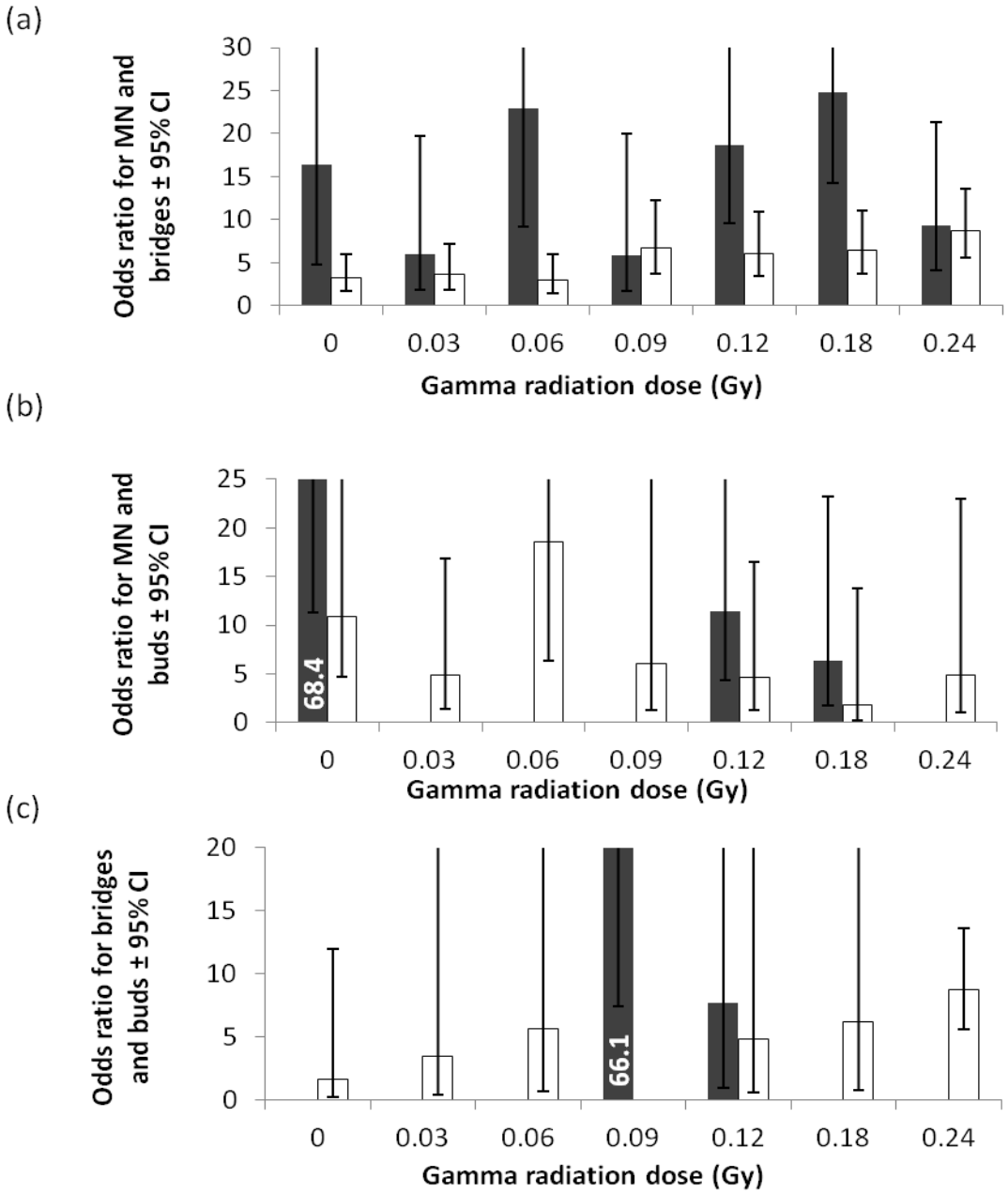

Figure 2.4 Odds ratios for the simultaneous presence (a) of micronuclei (MN) and nucleoplasmic bridges, (b) micronuclei and buds, and (c) bridges and buds in two normal human lymphoblastoid cell lines treated with low doses of γ-radiation from a Cobalt-60 source. Numbers inside the truncated bars indicate the value of that observation. Some upper confidence intervals have been truncated to provide a closer look at the data. Missing values at some doses indicate that the odds ratio could not be calculated due to a lack of cells containing one or both of the two endpoints being evaluated.

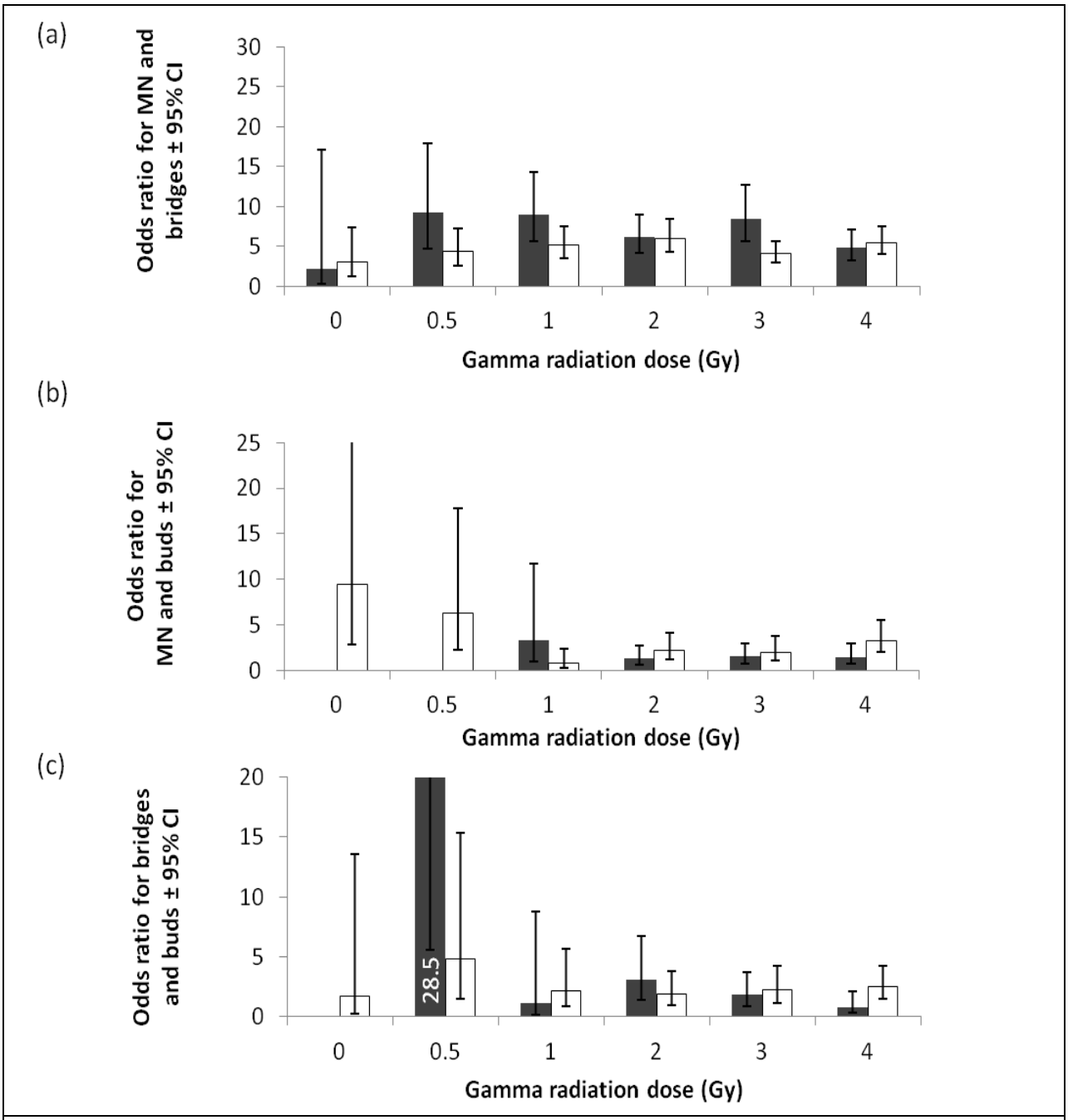

Figure 2.5 Odds ratios for the simultaneous presence (a) of micronuclei (MN) and nucleoplasmic bridges, (b) micronuclei and buds, and (c) bridges and buds in two normal human lymphoblastoid cell lines treated with high doses of γ-radiation from a Cobalt-60 source. Numbers inside the truncated bars indicate the value of that observation. Some upper confidence intervals have been truncated to provide a closer look at the data. Missing values at some doses indicate that the odds ratio could not be calculated due to a lack of cells containing one or both of the two endpoints being evaluated.

From a mechanistic standpoint, these observations may be explained by asymmetrical chromosome exchanges that result from the misrepair of DNA double-strand breaks, where each such event leads to rearrangements that generate an acentric chromosome fragment and a dicentric chromosome. Many of these dicentrics and fragments would emerge in the next metaphase as bridges and fragments, respectively, and the fragments could also appear in the next interphase as micronuclei. The breakage-fusion-bridge cycle, a mechanism of chromosome instability involving repeated cycles of fusion between chromosomes or chromatids and their subsequent breakage during cell division as centromeres separate [9, 24] has been proposed to explain the observation that the presence of micronuclei, bridges and buds are highly correlated in folic acid-deficient cells [11, 12]. The same is not likely in this experiment, as cells are treated with cytochalasin B four hours following irradiation, thus preventing cells from undergoing more than one cell division after the initial damage. Therefore, mechanisms other than the breakage-fusion-bridge cycle must be significant contributors in our observation of correlated increases in micronuclei, bridges and buds.

Our results suggest that not only do asymmetrical chromosome exchanges account for a fixed, observable proportion of the micronuclei and bridges generated by treatment with ionizing radiation, but also that the CBMN assay is capable of detecting such events. The frequency of micronuclei may provide an estimate of the number of acentric fragments produced in response to a treatment. Similarly, the frequency of nucleoplasmic bridges may be a reliable indicator of the number of dicentrics present [10]. By producing a calibration curve comparing the number of dicentric and acentric chromosomes from Giemsa-stained metaphase spreads to the micronuclei and bridge

frequencies induced in CBMN assay, it may be possible to predict the results of one assay without performing the other. Cells undergoing apoptosis and necrosis were not recorded in this study; these biomarkers may affect the relationships between micronuclei, buds and bridges. More studies are required to investigate this further.

Positive associations, as evaluated by odds ratios, also occurred for the presence of micronuclei and nuclear buds (Figure 2.3b, 2.4b, 2.5b), and for the presence of nucleoplasmic bridges and nuclear buds (Figure 2.3c, 2.4c, 2.5c) within each cell in cell lines treated with γ-radiation or neutron radiation. While it is known that certain types of micronuclei arise by nuclear budding, and that some buds arise from the breaking of bridges, it is unclear how these simple relationships would lead to an increased concurrent presence of buds with bridges or micronuclei in each cell. An alternative explanation is that certain cells within the cell population have increased susceptibility to DNA damage; variability in radiosensitivity of individual cells based on their phase in the cell cycle is known to occur [25]. Thus, the positive associations between the different endpoints in individual cells may be due (at least in part) to an increased frequency of radiation damage within this certain subset of cells [25].

Unlike the odds ratios between micronuclei and bridges, and between bridges and buds, the odds ratios for the presence of micronuclei and buds were found to be heterogeneous for 2 of the 6 treatment sets examined. This suggests that the association between micronuclei and buds is not static among various treatment conditions but may be dependent on radiation dose. However, it should also be cautioned that the visual means used to identify buds in the CBMN assay may allow mis-identification of a small number of micronuclei as buds, as micronuclei in contact

with cell nuclei may not easily be determined to be separate through visual means alone. Thus, the possibility remains that any statistical association involving buds could be due to micronuclei that were incorrectly identified as buds.

In conclusion, in cells treated with γ-radiation and neutron radiation, the occurrence of micronuclei, bridges and buds within individual cells are positively associated with each other. This suggests the existence of a common mechanism of generation for these endpoints by chromosomal damage and structural chromosome rearrangements. Differences in radiosensitivity of individual cells within the cell population according to their position in the cell cycle at the time of exposure may also be important. Altering the scoring criteria of the CBMN assay such that only binucleated cells with well-separated nuclei are counted, as opposed to counting all binucleated cells with non-overlapping nuclei, significantly increases the frequency of bridges observed. Regardless of the scoring method used, statistically significant associations among micronuclei, bridges, and buds have been demonstrated in the work described here.

REFERENCES

1. Fenech, M., The lymphocyte cytokinesis-block micronucleus cytome assay and its application in radiation biodosimetry. Health Phys, 2010. **98**(2): p. 234-43.
2. Kirsch-Volders, M., et al., The in vitro MN assay in 2011: origin and fate, biological significance, protocols, high throughput methodologies and toxicological relevance. Arch Toxicol, 2011. **85**(8): p. 873-99.
3. Shimizu, N., Molecular mechanisms of the origin of micronuclei from extrachromosomal elements. Mutagenesis, 2011. **26**(1): p. 119-23.
4. Hoffelder, D.R., et al., Resolution of anaphase bridges in cancer cells. Chromosoma, 2004. **112**(8): p. 389-97.
5. Eastmond, D.A. and J.D. Tucker, Identification of aneuploidy-inducing agents using cytokinesis-blocked human lymphocytes and an antikinetochore antibody. Environ Mol Mutagen, 1989. **13**(1): p. 34-43.
6. Fenech, M. and A.A. Morley, Kinetochore detection in micronuclei: an alternative method for measuring chromosome loss. Mutagenesis, 1989. **4**(2): p. 98-104.
7. Vral, A., H. Thierens, and L. De Ridder, In vitro micronucleus-centromere assay to detect radiation-damage induced by low doses in human lymphocytes. Int J Radiat Biol, 1997. **71**(1): p. 61-8.
8. Fenech, M., et al., Molecular mechanisms of micronucleus, nucleoplasmic bridge and nuclear bud formation in mammalian and human cells. Mutagenesis, 2011. **26**(1): p. 125-32.
9. Murnane, J.P., Telomere dysfunction and chromosome instability. Mutation research, 2012. **730**(1-2): p. 28-36.

10. Thomas, P., K. Umegaki, and M. Fenech, Nucleoplasmic bridges are a sensitive measure of chromosome rearrangement in the cytokinesis-block micronucleus assay. Mutagenesis, 2003. **18**(2): p. 187-94.

11. Crott, J.W., et al., The effect of folic acid deficiency and MTHFR C677T polymorphism on chromosome damage in human lymphocytes in vitro. Cancer Epidemiology, Biomarkers & Prevention, 2001. **10**(10): p. 1089-96.

12. Fenech, M. and J.W. Crott, Micronuclei, nucleoplasmic bridges and nuclear buds induced in folic acid deficient human lymphocytes-evidence for breakage-fusion-bridge cycles in the cytokinesis-block micronucleus assay. Mutation Research, 2002. **504**(1-2): p. 131-6.

13. Utani, K., A. Okamoto, and N. Shimizu, Generation of micronuclei during interphase by coupling between cytoplasmic membrane blebbing and nuclear budding. PLoS One, 2011. **6**(11): p. e27233.

14. Utani, K., et al., Emergence of micronuclei and their effects on the fate of cells under replication stress. PLoS One, 2010. **5**(4): p. e10089.

15. Serrano-Garcia, L. and R. Montero-Montoya, Micronuclei and chromatid buds are the result of related genotoxic events. Environ Mol Mutagen, 2001. **38**(1): p. 38-45.

16. Fenech, M. and A.A. Morley, Measurement of micronuclei in lymphocytes. Mutat Res, 1985. **147**(1-2): p. 29-36.

17. Hovhannisyan, G., R. Aroutiounian, and T. Liehr, Chromosomal composition of micronuclei in human leukocytes exposed to mitomycin C. J Histochem Cytochem, 2012. **60**(4): p. 316-22.

18. Asur, R.S., R.A. Thomas, and J.D. Tucker, Chemical induction of the bystander effect in normal human lymphoblastoid cells. Mutat Res, 2009. **676**(1-2): p. 11-6.

19. Fenech, M., et al., HUMN project: detailed description of the scoring criteria for the cytokinesis-block micronucleus assay using isolated human lymphocyte cultures. Mutation Research, 2003. **534**(1-2): p. 65-75.

20. Fenech, M., Cytokinesis-block micronucleus cytome assay. Nature Protocols, 2007. **2**(5): p. 1084-104.

21. Woolf, B., On estimating the relation between blood group and disease. Ann Hum Genet, 1955. **19**(4): p. 251-3.

22. Mantel, N. and W. Haenszel, Statistical aspects of the analysis of data from retrospective studies of disease. J Natl Cancer Inst, 1959. **22**(4): p. 719-48.

23. Rajendran, S., et al., The role of mitochondria in the radiation-induced bystander effect in human lymphoblastoid cells. Radiat Res, 2011. **175**(2): p. 159-71.

24. McClintock, B., The Stability of Broken Ends of Chromosomes in Zea Mays. Genetics, 1941. **26**(2): p. 234-82.

25. Pawlik, T.M. and K. Keyomarsi, Role of cell cycle in mediating sensitivity to radiotherapy. Int J Radiat Oncol Biol Phys, 2004. **59**(4): p. 928-42.

CHAPTER 3

This chapter has been published in the journal "PLOS ONE". The citation of this paper is:

Seth, I., Schwartz, J.L., Stewart, R.D., Emery, R., Joiner, M.C., Tucker, J.D. (2014) Neutron exposures in human cells: bystander effect and relative biological effectiveness, PLOS ONE Vol 9 (6): e98947.

Neutron exposures in human cells: bystander effect and relative biological effectiveness

INTRODUCTION

Ionizing radiation leads to chromosome damage of the type seen in cancer cells. Ionizing radiation is also an effective method for treating tumors because it can be localized to the tumor and is a potent inducer of DNA double-strand breaks, a highly toxic form of DNA damage. While much has been learned about x-ray and gamma-ray effects on cells and whole organisms, less is known about the biological effects of neutrons. Neutrons are highly energetic uncharged particles that induce more severe DNA damage than photons and are therefore more effective than photons in controlling radioresistant tumors. The relative biological effectiveness (RBE) of neutrons has been reported to be as low as 1 and perhaps higher than 10 depending on the tissue type, neutron energy and the biological endpoint being measured [1]. Neutrons were listed as a carcinogen for the first time in the Eleventh Report on Carcinogens [2]. High levels of neutron irradiation occur in patients receiving neutron therapy, while low levels of neutron exposure occur in patients treated with high energy photons and protons. Other

sources of low level neutron irradiation may include occupational exposure to workers at nuclear power plants and accelerator facilities, astronauts, airline crews and passengers on high altitude flights [3-14], as well as radiation incidents such as the Hiroshima-Nagasaki atomic bomb explosions and the tsunami-induced radiation leak at the Fukushima Daiichi site in Japan [15].

One of the major paradigm shifts in the field of radiation biology was the discovery of non-targeted effects such as the bystander effect in which cells in the vicinity of radiation-damaged cells behave as though they were also irradiated [16-20]. In addition, late effects such as chromosomal instability may increase susceptibility to cancer [21]. Thus, cells that are directly damaged are not the sole targets of radiation exposure. Cells that do not absorb radiation directly may nevertheless be damaged or altered in ways that do not become apparent for many cell generations. Such non-targeted effects may have serious implications for human health and may cause cancer. Therefore, the risks of ionizing radiation need to be analyzed in terms of both direct and non-targeted effects.

The bystander effect has been observed repeatedly in mammalian cell lines, including human skin fibroblasts, epithelial cells and leukemic cells in response to ionizing photons [17,22-36]. Depending upon the cell and tissue type, bystander signals can be transmitted either through the culture medium [17] or by cell-to-cell contact including gap junctional communication [37]. Some of the candidate intercellular signaling molecules that have been implicated in bystander effects are reactive oxygen species [20,38], reactive nitrogen species [20,38], nitric oxide [27,38], cytokines such as TGFβ and interleukin 8 [39], and small molecules such as amino acids [37,40,41]. The

involvement of intracellular signaling molecules including mitogen-activated protein kinases (MAPK) and their downstream proteins [42,43], protein kinase C (PKC) isoforms [44], tumor protein 53 (p53) [45,46], cyclin-dependent kinase inhibitor 1A (CDKN1A, p21) [47], ataxia telangiectasia mutated protein (ATM) [44], and ataxia telangiectasia and Rad3 related (ATR) DNA-dependent protein kinase (DNA-PK) [44,48] have also been implicated. Recently, some laboratories have suggested that the presence of serotonin in the serum is one of the key factors involved in the bystander effect [49-51], however this finding has been disputed [52].

Most bystander effect studies have been performed using x-rays [22,24,29], gamma rays [17,35,53] and alpha particles [47,54,55], however, little has been done concerning the effects of neutron radiation [56]. Such information might be important for risk estimation in response to neutron exposure. No conclusive cytogenetic evidence exists to support or refute the existence of non-targeted effects in cellular responses to neutrons. A bystander effect following neutron exposure has been observed in Chinese hamster ovary cells [57], but no effect was seen in zebrafish irradiated *in vivo* [56]. There are no available cytogenetic data concerning the bystander effect in human cells in response to neutrons.

Here we used the cytokinesis-block micronucleus assay to address the question whether neutrons induce a bystander effect in normal human lymphoblastoid cell lines. We also assessed the RBE of fast neutrons produced by 50.5 MeV protons incident on a Be target (~17 MeV average neutron energy) compared to cobalt-60 gamma radiation. For the endpoints of micronuclei and nucleoplasmic bridges, we found no evidence to indicate that neutrons induce a bystander effect in normal human lymphoblastoid cells.

The measurements indicate that the neutron RBE for directly damaged cells compared to cobalt-60 gamma rays is 2.0 ± 0.13 for micronuclei and 5.8 ± 2.9 for bridges.

MATERIALS AND METHODS

Cell lines

Normal human lymphoblastoid cell lines (GM15036 and GM15510) obtained from the Coriell Cell Repository were used for these experiments because they have previously been shown to exhibit a bystander effect in response to gamma radiation [22,24].

Cell culture

Cell culture was performed using the standardized protocol provided by Coriell. The serum used in this study was prescreened for its ability to support a bystander effect with the cytokinesis-block micronucleus assay in these same cell lines. Since serotonin has been reported to play a role in the bystander effect [49] and is light sensitive, the bottles containing the culture media were wrapped in aluminum foil and stored in the dark. Cells were cultured and grown in suspension in non-vented T-25 flasks with loosened caps (Corning, NY and ISC BioExpress, Kaysville, UT) containing 10 ml of medium consisting of RPMI1640 (GIBCO, Grand Island, NY or Hyclone, Logan, UT) supplemented with 15% Fetal Bovine Serum (FBS, Atlanta Biologicals, Lawrenceville, GA), 2 mM L-glutamine (GIBCO, Grand Island, NY), penicillin-streptomycin (100 units/ml penicillin G Sodium, 100 µg/ml Streptomycin sulfate in 0.85% saline; GIBCO, Grand Island, NY), fungizone (amphotericin B, 2.5 µg/ml, 0.2 µm filtered; Hyclone, Logan, UT). All cultures were grown and maintained in a fully humidified 5% CO_2 incubator at 37°C. Approximately every 3 days the cells were

counted and passaged by seeding at a concentration of $3x10^5$ cells/ml. Cell culture for all the gamma radiation experiments was performed at Wayne State University (WSU), Detroit, Michigan. For the neutron radiation experiments, cells were grown at WSU up to a concentration of $1x10^6$ cells/mL, then non-vented T-25 flasks were completely filled with media (60 ml) containing cells at this concentration. Two flasks per cell line were then shipped overnight to the University of Washington Medical Center (UWMC), Seattle. Upon arrival, the flasks were immediately placed upright in a fully humidified 5% CO_2 incubator at 37°C, and their caps were loosened. The flasks were left undisturbed for 24 hours after which the cells were counted and checked for viability using a hemocytometer and trypan blue staining. Cells were then passaged once and cultured as described above.

Radiation exposures

All neutron irradiations were carried out using the fast clinical neutron therapy system (CNTS) at the University of Washington (Seattle, WA). All gamma irradiations were performed in the Gershenson Radiation Oncology Center, WSU. For neutron irradiations, the cells in culture medium in T-25 flasks were irradiated at room temperature with doses 0 (sham), 0.5, 1, 1.5, 2, 3 and 4 Gy. The CNTS generates fast neutrons by targeting a near monoenergetic 50.5 MeV proton beam at a Be target (10.5 mm thick with a radius of 0.635 cm). The neutron beam is shaped by a primary collimator composed of iron and a secondary collimator made up of individually movable leaves composed of iron with cylindrical polyethylene inserts. Cells in T-25 flasks with

culture medium were placed on top of 2 cm of water-equivalent material and irradiated at 0.6 Gy/min from below (gantry at 180 degree) using an open 28.8 x 28.8 cm^2 field (SSD of 148 cm). The average energy and neutron mean free path varies with field size and water-equivalent depth (nominal depth of maximum dose is 1.5 cm). For experiments reported in this work, the average neutron energy is about 17 MeV, and the neutron mean free path in water is about 9 cm. For every dose, two flasks were irradiated per cell line: one flask was used to assess the damage induced by direct radiation exposure and the other flask was used for medium transfer for the bystander effect as described below. For the direct damage and the bystander effect experiments, three different controls were used: pre-radiation, post-radiation, and transportation control. Pre-radiation and post-radiation control flasks were sham-irradiated with exposure times corresponding to the lowest (0.5 Gy) and the highest (4 Gy) neutron dose, respectively. The transportation control involved flasks that were transported with the cells that were irradiated, but remained inside the insulated box; these control flasks were further insulated with bubble wrap to maintain their temperature close to 37°C. This box was the same as that used to carry the flasks to and from the laboratory and the radiation center (a 2 minute walk). For the bystander effect an additional media-only control was included; these flasks contained fresh, complete, culture media without any cells and were irradiated at the highest dose, i.e. 4 Gy. Media from these flasks was transferred to non-irradiated cells in the same manner as described for media transfer from flasks that contained cells. Following exposure the flasks were returned immediately to the laboratory and incubated for 28 hours. The cells were then harvested as described below. For each cell line, the neutron bystander experiment was

performed twice, once each on different days. Replicate 2 had all the controls as described for replicate 1 except the transportation control was not included.

The Be target system used to generate fast neutrons also delivers a photon dose of about 5% of the neutron dose, which raises the possibility that any bystander effect observed in the experiments could be due to photons rather than to the neutrons. To rule out this possibility, cells were acutely irradiated with cobalt-60 gamma rays at doses equivalent to the 5% of the delivered neutron dose, i.e. 0 (sham), 0.025, 0.05, 0.075, 0.10, 0.15 and 0.20 Gy. We also included a media-only control containing fresh media without cells, which was irradiated at the highest dose, i.e. 0.2 Gy.

As a positive control for the bystander effect, cells were exposed to 0 (sham), 0.5, 1, 2, 3 and 4 Gy cobalt-60 gamma rays. To ensure that the bystander effect observed was actually due to signals produced by the irradiated cells rather than an effect of exposure of the culture medium or an artifact of the media transfer process, a media-only control was included in which fresh media without cells was irradiated at the highest dose (4 Gy) prior to being transferred to non-irradiated cells. For the gamma radiation experiments, flasks were transported to and from the laboratory and the radiation center, a 5-minute car ride, in an insulated container as described above.

Assessment of direct radiation damage

To assess the effects of direct radiation damage on these cells, Cytochalasin B (6 µg/ml final concentration; Sigma, St. Louis, MO) dissolved in DMSO (Fisher Scientific, Pittsburg, PA) was added four hours after irradiation to directly-irradiated cells

to block cytokinesis. The final concentration of DMSO in each culture was 1.1%. The cell cultures were then incubated at 37°C for 28 hours.

Media transfer

Following irradiation, the cells were left undisturbed until media transfer, which was performed four hours after irradiation as previously described [17]. Briefly, the cell cultures from the non-irradiated and irradiated flasks were transferred to 15 ml centrifuge tubes (Nalgene Nunc International, Rochester, NY) and centrifuged at 370 x g for 5 minutes. To ensure that no cells were transferred along with the media, the supernatant was then passed through 0.22 µm polyethylsulfonate syringe filters (Nalgene). The media from the irradiated cells contains factors secreted by the irradiated cells and hence is considered to be “conditioned”. The media from the non-irradiated (bystander) cells was gently removed by aspiration and replaced with conditioned media. The non-irradiated cells in the conditioned media were then transferred to new T-25 culture flasks and immediately after media transfer 6 µg/ml (final concentration) of Cytochalasin B was added to each culture to block cytokinesis. The cell cultures were then incubated at 37°C for 28 hours.

Micronucleus Assay - Cell harvesting and slide preparation

Twenty-eight hours following media transfer, the cultures were swirled and pipetted gently to resuspend and break up the clumps of cells. Cells that were directly irradiated as well as those treated with conditioned media were centrifuged onto ethanol-cleaned microscope slides for 4 minutes at 93 x g using a cytocentrifuge

(Statspin, Westwood, MA). The slides were air-dried, fixed in 100% methanol (Fisher Scientific Pittsburgh, PA) for 15 minutes, and then stained with 100 µl of acridine orange (0.5 mg/ml in 1X PBS) (Allied Chemical Corporation, Morristown, NJ) for 1 minute in the dark. The excess stain was removed by washing in 1X PBS for 1 minute. The slides were then mounted with 1X PBS and 25 x 25 mm^2 glass coverslips.

Micronuclei scoring criteria

All slides were coded prior to scoring to prevent observer bias. The Nuclear Division Index (NDI) for each dose and treatment was determined by evaluating at least 200 cells and determined according to the following formula:

$$NDI = [(M1 + (2 \times M2) + (3 \times M3) + (4 \times M4)) / N]$$

where M1-M4 represent the number of cells with one to four nuclei, respectively, and N is the total number of cells scored [75]. Calculation of the NDI was important to ensure that the number of binucleated cells was sufficient for enumerating micronuclei.

Cells were then evaluated simultaneously for micronuclei, nucleoplasmic bridges and buds according to our “relaxed” criteria [76]. Briefly, only binucleated cells with non-overlapping nuclei were evaluated. Micronuclei were required to be no more than one-third the size of the nuclei, and to be round or oval with smooth edges and stained the same color as the nuclei. Bridges were required to span the entire distance between the two nuclei. Buds were counted only if the stalk was thinner than the widest part of the bud. Since buds did not exhibit a consistent response for either cell line in any of the

experiments, we have not included these data in this paper. For each treatment condition, at least 1000 binucleated cells were scored by trained observers. For any experiment, either one observer evaluated all the treatment conditions or the scoring was balanced between two observers such that each evaluated approximately equal numbers of cells for each treatment condition.

Statistical Analyses

Analysis of variance (ANOVA) was performed to evaluate radiation-induced dose responses in cells directly irradiated with neutrons or high doses of photons, and in cells treated with ICCM from these irradiated cells. For each experiment, the independent variables considered were cell line, dose, and the interaction between cell line and dose. The dependent variables were micronuclei and bridges. The same set of analyses were performed for the neutron bystander data which included replicate experiments as an additional variable. The Tukey HSD test was used for post-hoc evaluations. These analyses were performed using JMP software version 6.0, SAS Institute Inc. Chi squared analyses were used to evaluate changes in the frequencies of micronuclei and bridges in the irradiated cells as a pooled group compared to the unirradiated (0-dose control) cells for the high dose photon experiments, and for the low dose photon contamination experiments.

RESULTS

Nuclear Division Indices

The Nuclear Division Indices (NDI) for all experimental conditions were high enough to enumerate micronuclei and bridges, with the exception of cells irradiated with the highest two neutron doses (3 Gy and 4 Gy). Here, radiation-induced cell cycle delays precluded obtaining sufficient numbers of scoreable binucleated cells (Table 1). Although these cells had NDI values similar to the 3 Gy and 4 Gy photon-irradiated cells, they could not be scored because their morphology was not compatible with accurate damage assessments. NDI's for the two replicate neutron bystander experiments were very similar ($p > 0.05$).

Table 3.1. Average number of nuclei per cell in directly exposed and bystander cells for neutron and cobalt-60 gamma rays.

Radiation dose (Gy)	Nuclear division index			
	GM15510 cells		GM15036 cells	
	Direct	Bystander[a]	Direct	Bystander[a]
Neutrons				
0 (pooled)[b]	2.27	2.11	1.98	2.11
4 (media only)[c]	-	2.23	-	2.09
0.5	1.61	2.20	1.39	2.00
1	1.46	2.06	1.40	1.98
1.5	1.35	1.90	1.25	2.33
2	1.24	2.18	1.18	1.93
3	1.20[d]	2.07	1.14[d]	2.13
4	1.11[d]	2.30	1.09[d]	2.14
Cobalt-60 γ				
0	1.92	1.79	1.79	1.71
4 (media only)[c]	-	1.97	-	1.83
0.5	1.87	1.89	1.58	1.79
1	1.64	1.92	1.51	1.93
2	1.24	1.82	1.21	1.81
3	1.13	1.92	1.19	1.82
4	1.06	1.90	1.13	1.85

[a] Neutron data shown are for replicate 1; the values for replicate 2 were similar ($p > 0.05$).

[b] Combined values of the controls (pre-radiation, post-radiation and transportation control).

[c] Media without cells was irradiated with 4 Gy and transferred to unirradiated cells.

[d] Too few high quality binucleated cells were available for scoring.

Direct damage induced by neutrons

For both cell lines, direct irradiation with neutrons resulted in clear dose-responsive increases in the number of micronuclei (Figure 3.1a) and nucleoplasmic bridges (Figure 3.1b) per 1000 binucleated cells. Since the three 0-dose controls (i.e., pre-radiation, post-radiation, and transportation control) for micronuclei and for nucleoplasmic bridges were not statistically different from each other as determined by ANOVA, we report only the pooled control values for these endpoints.

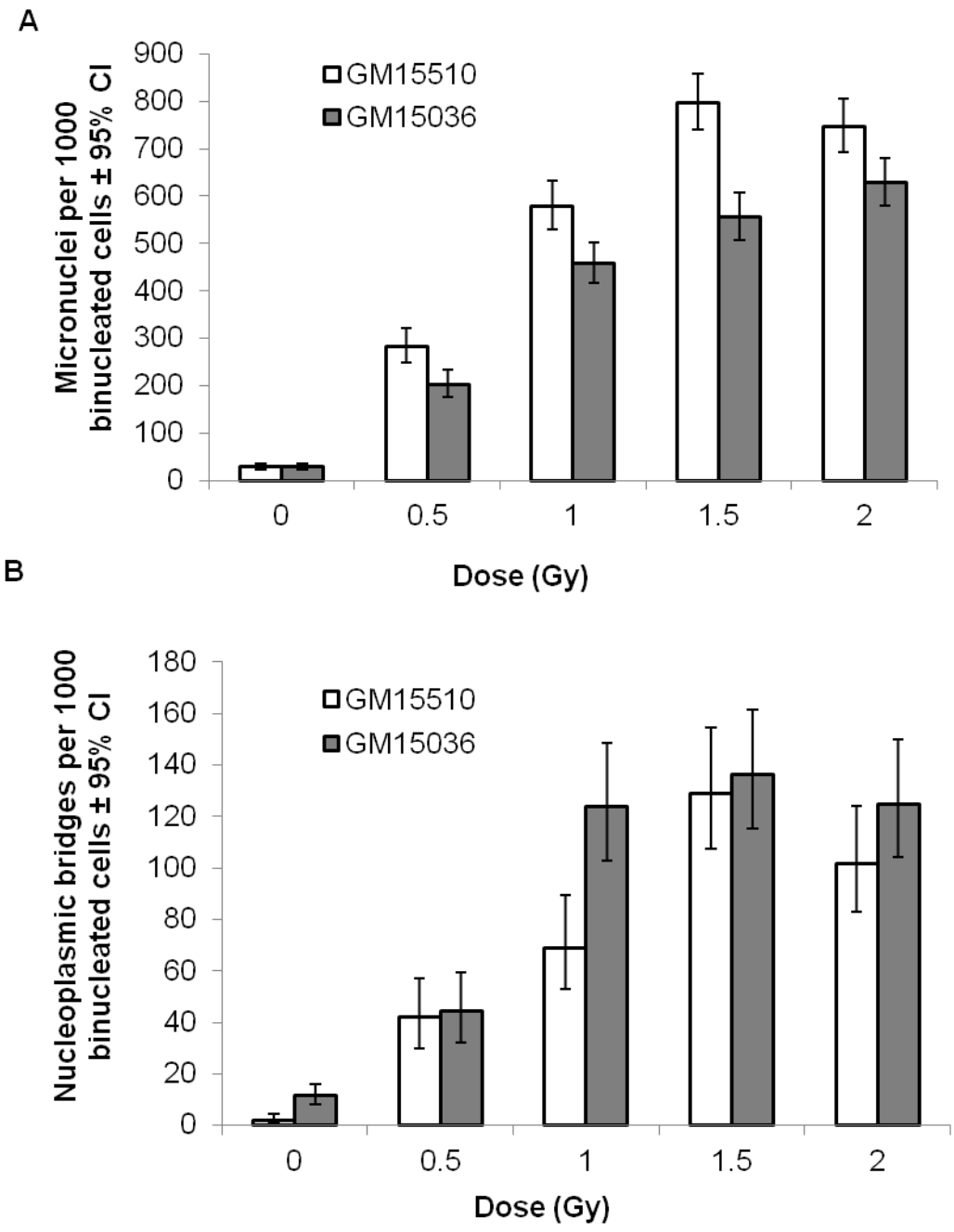

Figure 3.1 Micronuclei (a) and nucleoplasmic bridges (b) per 1000 binucleated cells in normal human lymphoblastoid cells directly irradiated with neutrons. Vertical lines represent the 95% confidence intervals.

Lack of bystander effect in response to neutrons

Cells treated with ICCM from neutron irradiated cells did not show significant increases in micronuclei frequencies compared to sham treated controls for either replicate experiment and for either cell line (Figure 3.2). As expected, the media-only control and the 0 Gy control were not statistically different ($p > 0.05$). For GM15510 cells, although the micronuclei frequencies show substantial variation, there clearly is not any consistent evidence of a bystander effect. GM15036 cells that received ICCM from any dose greater than 0 had frequencies of micronuclei that were similar to each other, and all were lower than the 0-dose values, although the differences were not statistically significant. The frequencies of nucleoplasmic bridges (Figure 3.2b) showed considerable variation and no consistent dose-related response was seen for either cell line. For both cell lines and for both end-points, i.e. micronuclei and nucleoplasmic bridges, compared to the controls no treatment condition caused any statistically significant change in the frequencies for either of the replicate experiments ($p > 0.05$). These data indicate that neutrons do not induce a bystander effect in these cell lines under these experimental conditions.

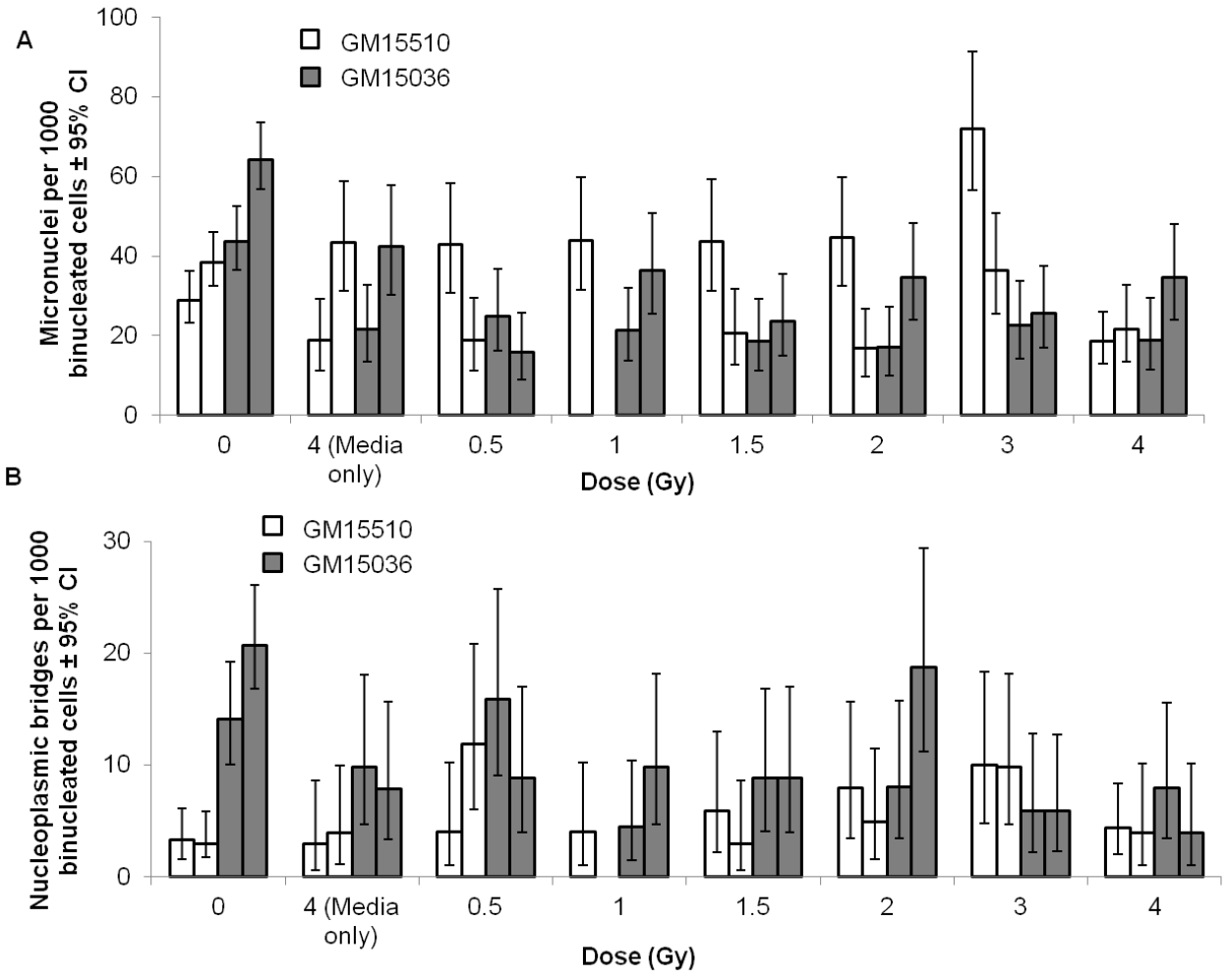

Figure 3.2 Micronuclei (a) and nucleoplasmic bridges (b) per 1000 binucleated cells in normal human lymphoblastoid cells cultured in conditioned media from neutron irradiated cells. For each treatment (i.e., cell line and dose group) the left-hand bar in each pair is replicate 1 and the right-hand bar is replicate 2. The 1 Gy data are missing for GM15510 cells replicate 2 because the sample was lost. Vertical lines represent the 95% confidence intervals.

No bystander effect observed due to photon contamination

The neutron beam used in these experiments is contaminated with photons at a level of approximately 5%. Even though a bystander effect was not observed with the neutron exposures, we sought to determine whether photons might cause a bystander effect at the doses employed in these experiments. We cultured GM15510 and GM15036 cells in ICCM obtained from the corresponding cell line that had been irradiated with cobalt-60 at doses equivalent to 5% of the neutron doses. The results, shown in Figure 3.3, indicate that these low doses of photons did not produce a bystander effect. As a pooled group, cells grown in ICCM showed no significant increase in the frequencies of micronuclei or bridges compared to cells grown in conditioned media from unirradiated cells, as determined by Chi-squared analyses. The media-only control had values similar to the 0 Gy (control) for both endpoints.

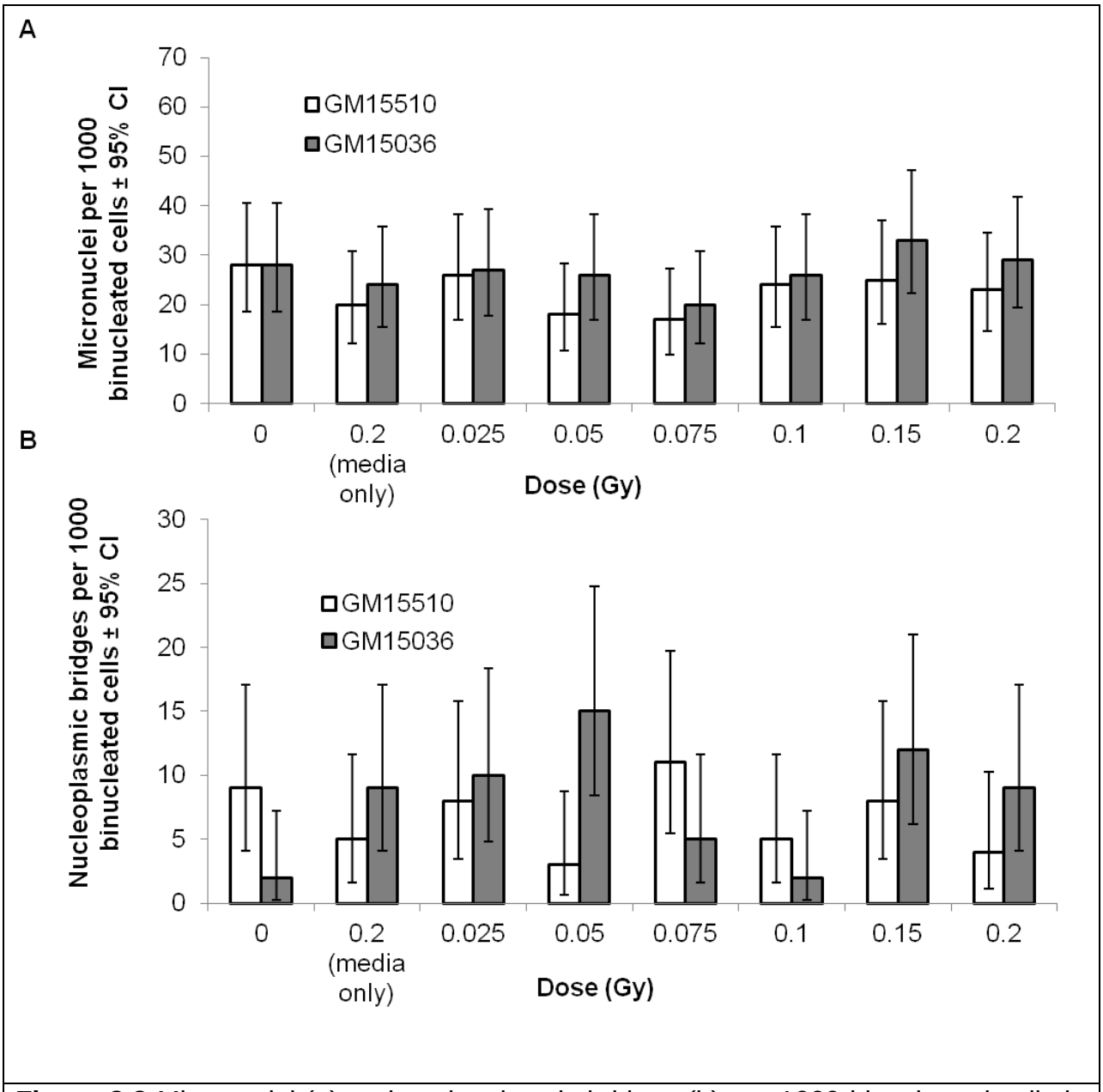

Figure 3.3 Micronuclei (a) and nucleoplasmic bridges (b) per 1000 binucleated cells in normal human lymphoblastoid cells treated with conditioned media from cells that were directly irradiated with cobalt-60 γ-radiation at doses equivalent to 5% of the neutron doses. Vertical lines represent the 95% confidence intervals.

Positive control experiment: Direct damage induced by high doses of cobalt-60 gamma rays

To reaffirm that the experimental conditions used here are capable of seeing a direct (i.e. non-bystander) effect of gamma ray exposure, experiments identical to those performed with neutrons were carried out with high doses of cobalt-60. Direct exposure to these photons with doses from 0 to 4 Gy showed a clear dose responsive increase in the number of micronuclei and the number of bridges per 1000 binucleated cells for both cell lines (Figure 3.4). The frequencies of micronuclei and bridges appear to saturate at higher doses, indicating that multiple chromosome fragments were packaged in some micronuclei, and that more than one dicentric might have contributed to some bridges. The increases for both micronuclei and bridges with dose were significant with and without considering the 4 Gy data point ($p < 0.0001$).

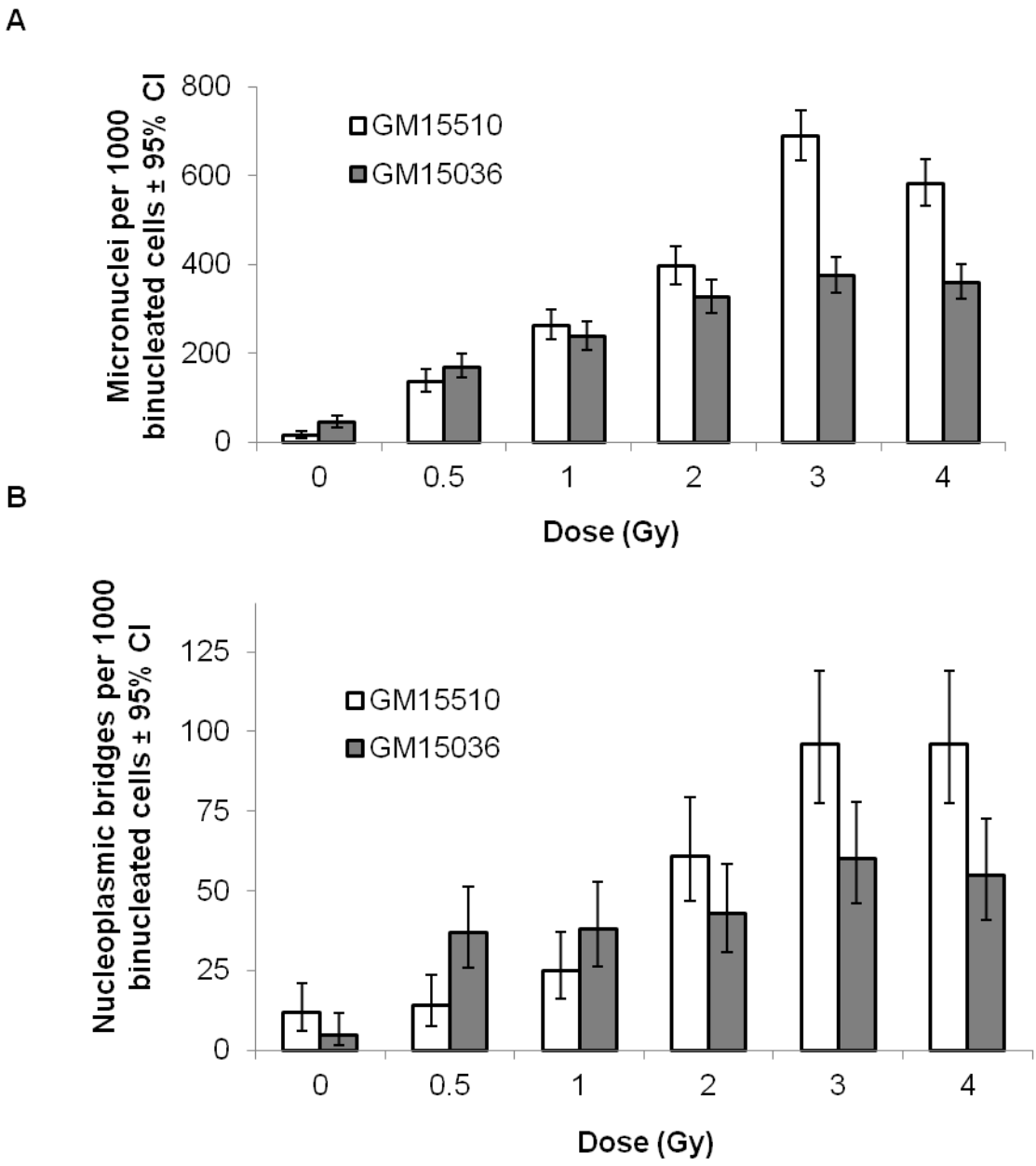

Figure 3.4 Micronuclei (a) and nucleoplasmic bridges (b) per 1000 binucleated cells in normal human lymphoblastoid cells directly irradiated with high doses of cobalt-60 γ-radiation gamma rays. Vertical lines represent the 95% confidence intervals.

Bystander effect induced by high doses of cobalt-60 gamma rays

Photons have been known to induce bystander effects in human cells for many years. However, since the neutron exposures and the low-dose photon exposures did not induce a bystander effect, it was important to verify that the cells and the experimental conditions in these experiments, including the serum used in the culture media, are capable of demonstrating a bystander effect if one exists. As expected, GM15510 and GM15036 cells cultured in ICCM obtained from cells exposed to high doses of cobalt-60 gamma rays showed a 2 to 3 fold increase in micronuclei frequencies compared to sham treated controls, clearly indicating induction of a bystander effect (Figure 3.5a). Compared to cells grown in conditioned media from unirradiated cells, as a pooled group all 6 ICCM cultures for each cell line showed increases in micronuclei ($p < 0.0001$). Nucleoplasmic bridges (Figure 3.5b) showed a weak bystander effect for GM15510 ($p = 0.052$), and for GM15036 the effect was highly significant ($p < 0.0001$).

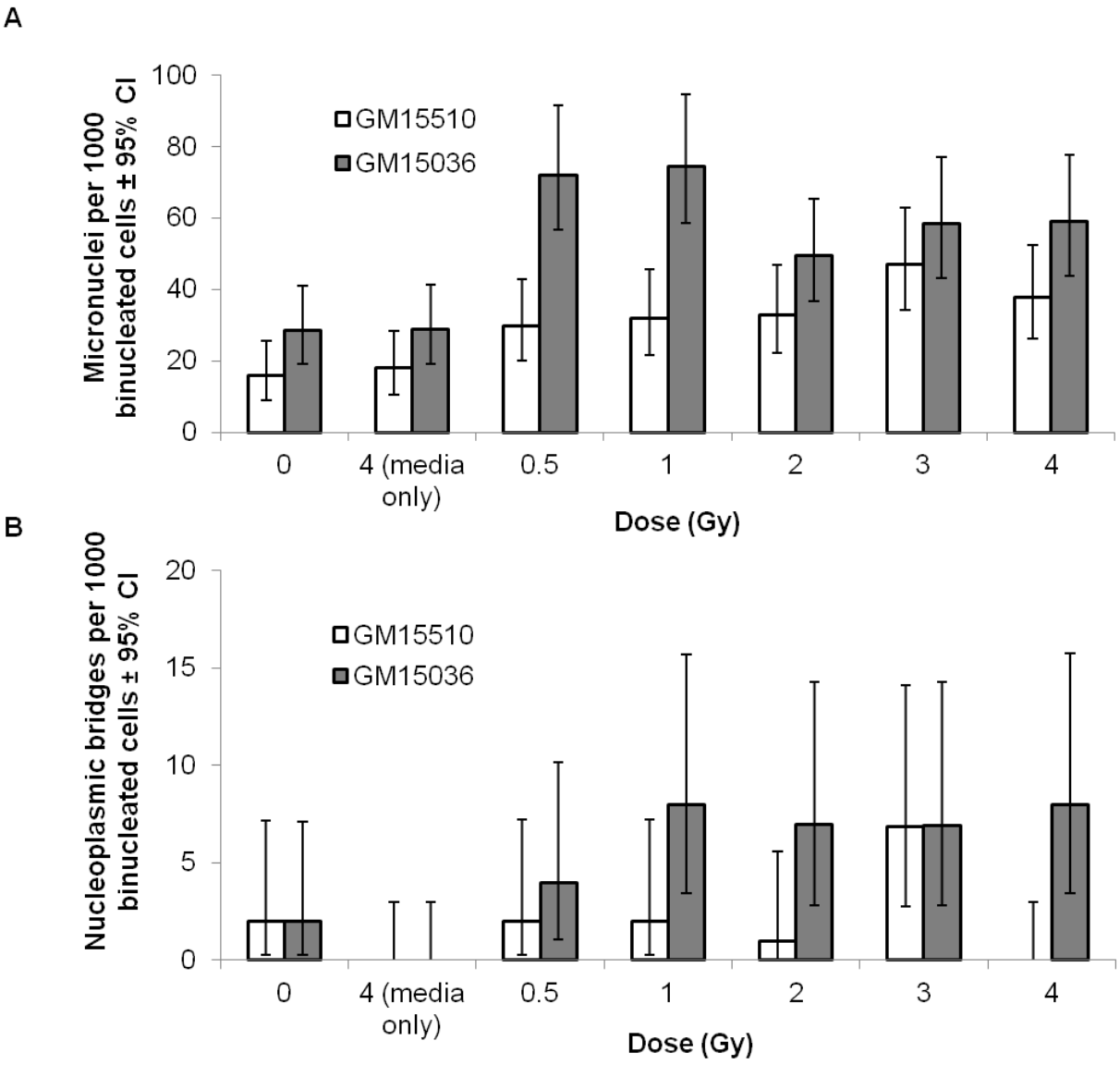

Figure 3.5 Micronuclei (a) and nucleoplasmic bridges (b) per 1000 binucleated cells in normal human lymphoblastoid cells cultured in conditioned media from cobalt-60 γ-irradiated cells. No bridges were observed in the 4 Gy sample for GM15510 cells, or for the media only samples for either cell line. Vertical lines represent the 95% confidence intervals.

Bystander component of the total dose response of cobalt-60 gamma rays and neutrons

If the mechanisms of action for direct and non-targeted damage are independent, the total cellular response to ionizing radiation is the sum of the direct and the indirect exposure effects. The bystander components in the total dose response of cobalt-60 gamma rays ranged from approximately 4% to 35% for micronuclei; for bridges, the bystander components ranged up to 6% for GM15510 cells and up to 23% for GM15036 cells (Tables 2 and 3). In contrast, there was no statistically significant bystander component for neutrons (data not shown).

Table 3.2. Percent contribution of the bystander effect to the total direct exposure effect in cobalt-60 irradiated cells for micronuclei.

Cobalt-60 gamma dose (Gy)	Micronuclei/1000 binucleated cells		Micronuclei induced[a]		% bystander component [b]
	Direct exposure	Bystander exposure	Direct exposure	Bystander exposure	
GM15510 cells					
0	15.0	15.9	0.0	0.0	
0.5	136.0	29.9	121.0	14.0	11.6
1.0	262.0	31.9	247.0	16.0	6.5
2.0	396.0	32.9	381.0	17.0	4.5
3.0	688.0	47.0	673.0	31.1	4.6
4.0	583.0	37.8	568.0	21.9	3.9
GM15036 cells					
0	45.0	28.5	0.0	0.0	
0.5	169.0	72.2	124.0	43.7	35.3
1.0	237.0	74.6	192.0	46.2	24.0
2.0	327.0	49.6	282.0	21.1	7.5
3.0	375.0	58.4	330.0	30.0	9.1
4.0	359.0	59.0	314.0	30.5	9.7

[a] Number of micronuclei per 1000 binucleated cells after subtracting the baseline (0 dose) values for that cell line.

[b] Percent of the induced total direct exposure response that can be attributed to the induced bystander effect.

Table 3.3. Percent contribution of the bystander effect to the total direct exposure effect in cobalt-60 irradiated cells for nucleoplasmic bridges.

Cobalt-60 gamma dose (Gy)	Bridges/1000 binucleated cells		Bridges induced[a]		% bystander component [b]
	Direct exposure	Bystander exposure	Direct exposure	Bystander exposure	
GM15510 cells					
0	12.0	2.0	0.0	0.0	
0.5	14.0	2.0	2.0	0.0	0.2
1.0	25.0	2.0	13.0	0.0	0.0
2.0	61.0	1.0	49.0	-1.0	–[c]
3.0	96.0	6.9	84.0	4.9	5.8
4.0	96.0	0.0	84.0	-2.0	–[c]
GM15036 cells					
0	5.0	2.0	0.0	0.0	
0.5	37.0	4.0	25.0	2.0	7.9
1.0	38.0	8.0	26.0	6.0	23.0
2.0	43.0	6.9	31.0	4.9	16.0
3.0	60.0	6.9	48.0	4.9	10.3
4.0	55.0	8.0	43.0	6.0	14.0

[a] Number of bridges per 1000 binucleated cells after subtracting the baseline (0 dose) values for that cell line.

[b] Percent of the induced total direct exposure response that can be attributed to the induced bystander effect.

[c] Percent bystander component could not be evaluated because the induced bystander effect is negative.

Relative biological effectiveness (RBE) of the UW CNTS Fast Neutrons

RBE is the ratio of doses that achieve the same biological effect for two radiation types. When the biological responses for both radiation types are linearly related to dose, as seen here, the RBE is also the ratio of the biological effects at the same dose. Here, the neutron RBE was calculated relative to cobalt-60 gamma rays by dividing the frequencies of micronuclei and bridges obtained in cells irradiated directly with neutrons at each dose to the frequencies obtained in cells irradiated directly with photons at the same dose. The RBE of neutrons for all doses and both cell lines is 2.0 ± 0.13 for micronuclei and 5.8 ± 2.9 for bridges (Table 4), indicating that neutrons are 2 to nearly 6 times more effective in damaging these cells compared to cobalt-60 gamma rays.

Table 3.4. Relative biological effectiveness for neutrons relative to cobalt-60 gamma rays for micronuclei and nucleoplasmic bridges.

Dose (in Gy)	Induced[a] micronuclei/1000 binucleated cells		RBE[b]	Induced[a] bridges/1000 binucleated cells		RBE[b]
	Cobalt-60 gamma rays	Neutrons		Cobalt-60 gamma rays	Neutrons	
GM15510 cells						
0	0.0	0[c]		0.0	0[c]	
0.5	121.0	255.0	2.1	2.0	40.0	20.0
1.0	247.0	551.4	2.2	13.0	66.9	5.1
2.0	381.0	718.8	1.9	49.0	99.7	2.0
GM15036 cells						
0	0.0	0[c]		0.0	0[c]	
0.5	124.0	173.0	1.4	32.0	32.8	1.0
1.0	192.0	427.9	2.2	33.0	112.0	3.4
2.0	282.0	599.3	2.1	38.0	113.3	3.0
mean +/- S.E. both cell lines			2.0 ± 0.13			5.8 ± 2.9

[a] The number of micronuclei or bridges per 1000 binucleated cells after subtracting the baseline (0 dose) values, which were 15.0 and 45.0 for micronuclei and 12.0 and 5.0 for bridges for cobalt-60 gamma for GM15510 and GM15036 cells, respectively. For neutrons the baseline values were 28.0 and 29.1 for micronuclei and 2.0 and 11.6 for bridges for GM15510 and GM15036 cells, respectively.

[b] Relative biological effectiveness: neutrons / cobalt-60 gamma rays.

[c] Combined values of the controls (pre-radiation, post-radiation and transportation control).

DISCUSSION

The experiments described here provide no cytogenetic evidence that fast neutrons are capable of inducing a bystander effect through medium-borne factors. The neutron beam used in these experiments was contaminated with photons, necessitating parallel evaluations to determine whether there is a positive or an inhibitory effect of these photons on the results of the neutron experiments. Our observation of an absence of a bystander effect following doses of photons that are associated with exposure to neutrons confirmed that there is a lack of a bystander effect in response to neutrons, regardless of the presence of photons. Wang et al. [56] have suggested that neutrons might suppress gamma ray-induced bystander signaling. They measured apoptosis and cell survival in zebrafish that received bystander signals from fish that were directly irradiated with neutrons. Since the doses of photons that contaminated these neutron exposures exceeded the minimum threshold for inducing a bystander effect [29,58], Wang et al. [56] suggested that the gamma ray-induced bystander effect might have been suppressed by the neutron exposures. With our data it is difficult to determine whether neutrons have the ability to suppress any bystander effect produced by photons because a source of uncontaminated neutrons is not available. The results shown here suggest that contaminating photons are not a likely confounding factor that interfered with the ability to detect a neutron-induced bystander effect.

Different responses to neutrons were observed in the two cell lines we used. GM15510 cells cultured in ICCM from neutron irradiated cells showed substantial variation in micronuclei frequencies but no consistent dose-related response. In contrast, GM15036 cells had micronuclei frequencies lower than the corresponding 0-

dose control value, although the control value was well within the historical range for this cell line. Although we did not measure apoptosis or necrosis, these outcomes may influence the responses seen in these cell lines.

There is clear evidence of a bystander effect in response to high doses of photons when we used the same serum and cell lines as for the neutron experiments. This result indicates that the methods used in our study are capable of detecting a bystander effect if such an effect exists. To the best of our knowledge there is no other factor that could have prevented neutrons from inducing a bystander effect in these cells, assuming a bystander effect even exists. Our findings are in agreement with previous studies that have reported the lack of a bystander effect on neutron exposure using clonogenic cell survival assay in a human skin cell line [29] and zebrafish [56]. However, other studies have reported contrasting results. Watson et al. [59] found that transplantation of a mixture of neutron irradiated and unirradiated bone marrow cells into mice induced instability in the descendants of unirradiated cells as confirmed by measuring chromosomal aberrations, indicating that neutrons induce a bystander effect. However, since the gamma component in neutrons was 25%, it is possible that the observed bystander effect was due to the contaminating photons, which the authors did not rule out. Kinashi et al. [57] studied a neutron-induced bystander effect in boron neutron capture therapy with a cell survival assay as well as cloning and sequencing methods. They reported an increase in the frequency of mutations in the hypoxanthine-guanine phosphoribosyltransferase locus in cells located near the irradiated cells. These results suggest that a neutron bystander effect may be comprised of gene mutations.

The inability of fast neutrons to induce a cytogenetic bystander effect as shown here may be due to different types of damage induced at the molecular level compared to photons. Cellular recognition of DNA damage and the subsequent repair processes may differ between neutrons and photons. Furthermore, due to the lower levels of oxidative damage and free radical production by neutrons compared to photons [60], some of the critical bystander signaling pathways may not be activated. There is also the possibility that a neutron-induced bystander effect, if any, might depend on cell type, the endpoint being evaluated [61,62], and the energy of the neutrons.

Neutrons, depending on their energy, might be more effective in controlling certain tumor types where conventional photon therapy is ineffective [63] because the oxygen enhancement ratio, i.e. the differential radiosensitivity between poorly oxygenated (more resistant) and well-oxygenated (more sensitive) cells, is reduced with neutrons. Unlike low-LET radiation, for high-LET radiation there is also a reduction in the differential radiosensitivity of cells related to their position in cell cycle [60]. Recently, radiation-induced bystander cells were shown to rescue irradiated cells through intercellular feedback. Chen et al. [40] observed a significant decrease in the number of DNA double-strand breaks, micronuclei frequencies, and the extent of apoptosis in irradiated cells that were co-cultured with unirradiated bystander cells. Observation of an absence of a bystander effect in the present study may help explain the sensitivity of radioresistant tumor cells to neutrons, because there is a possibility that the protection otherwise provided by the bystander effect on the tumor in response to neutrons is absent or not strong enough in magnitude, thereby causing tumor cells to be killed. The risks currently associated with neutron exposure may be over or underestimated

depending on which model of risk estimation is used to predict low dose risks from high dose data. Hence, reevaluation of radiation protection standards may be required. The work described in this paper may be relevant for radiation oncologists planning cancer treatments that involve fast neutron or proton radiotherapy, particularly for pediatric patients or pregnant women.

This study used cells that lack gap junctions. There is a possibility that a neutron-induced bystander effect requires physical contact between cells, which could be tested by performing experiments using cell lines such as fibroblasts and keratinocytes that have gap junctions. If no bystander effect is induced in these cell lines, then it may be likely that neutrons do not have any ability to induce a bystander effect. Another possible explanation for the lack of a bystander effect with neutrons observed in this study may be the presence of dimethyl sulfoxide (DMSO), a scavenger of reactive oxygen species [64,65], which was used to dissolve cytochalasin B that is required for the cytokinesis-block micronucleus assay. Both pre- and post-radiation treatment with DMSO is known to suppress DNA damage in irradiated cells [66]. However, this possibility seems unlikely in the work described here because we observed a bystander effect with an identical procedure involving DMSO when the same cell lines were exposed to photons. However, if a very small bystander effect was in fact induced by neutrons, then it may have been obscured by the DMSO, whereas the bystander effect induced by high levels of photons was too large to be masked by DMSO.

For cells irradiated with high doses of photons, a considerable amount of damage was attributed to the bystander component. The percent contribution by the bystander exposure to the direct exposure was highest at the lowest dose delivered (0.5

Gy) and then it appears to saturate as dose increases, perhaps because there is saturation either of the bystander signals or the cellular responses to those signals [67]. This observation is in agreement with other reports [55,68,69]. For cells irradiated with neutrons there is little or no damage that can be attributed to a bystander effect, because as previously noted, there is comparatively less oxidative damage following neutron than gamma exposure.

We report two RBEs for neutron radiation, one for micronuclei and the other for nucleoplasmic bridges. These two genetic endpoints have different mechanisms of formation. Micronuclei are formed from lagging chromosomes and acentric fragments at anaphase, while nucleoplasmic bridges are formed when centromeres of dicentric chromosomes are pulled in opposite directions during mitosis [70]. RBEs of 2.0 ± 0.13 for micronuclei and 5.8 ± 2.9 for nucleoplasmic bridges relative to cobalt-60 suggest that different kinds of genetic damage may be associated with different RBEs. RBE values are known to depend on factors such as linear energy transfer, tissue type, the extent of biological damage, and dose [60]. Knowing the RBE is important for radiation oncologists to determine the dose prescription and the most effective radiotherapy treatment plan for cancer patients. Yang et al. [71] reported RBEs of 2.35 and 2.42 for fast neutrons in immature rat hippocampal cells, as determined by two different cell viability assays. Dagrosa et al. [72] used the cytokinesis-block micronucleus assay and a cell survival assay in a human colon carcinoma cell line and observed an RBE of 4.4 for neutrons in boron neutron capture therapy. RBEs for neutrons as low as 4 to as high as 63 have been reported after measuring life-shortening responses in mice [73], apoptosis [1] and induction of dicentrics [74] in human lymphocytes. These numbers

clearly indicate that the RBEs for neutrons vary with the biological system, neutron energy and the end-point. Our RBE values are within the range of what others have reported.

In conclusion, we found no evidence for a bystander effect following exposure to fast neutrons (17 MeV average energy) or to doses of cobalt-60 photons equivalent to 5% of the neutron dose. As expected, a bystander effect was seen with high doses of photons, as evaluated by micronuclei frequencies and nucleoplasmic bridges. These results will facilitate refined estimates of the risk-benefit ratio of neutron therapy and may be valuable to those who are concerned about the health effects of exposure of space travel. We have also shown that these fast neutrons have a relative biological effectiveness of 2.0 ± 0.13 for micronuclei and 5.8 ± 2.9 for bridges compared to cobalt-60. Understanding the biological effects of neutrons may also enable more refined evaluations of the standards for radiation protection and safety.

REFERENCES

1. Ryan LA, Wilkins RC, McFarlane NM, Sung MM, McNamee JP, et al. (2006) Relative biological effectiveness of 280 keV neutrons for apoptosis in human lymphocytes. Health Phys 91: 68-75.

2. National Toxicology Program (2004) Report on Carcinogens, Eleventh Edition. National Toxicology Program.

3. Dietze G, Bartlett DT, Cool DA, Cucinotta FA, Jia X, et al. (2013) ICRP, 123. Assessment of radiation exposure of astronauts in space. ICRP Publication 123. Ann ICRP 42: 1-339.

4. Perez-Andujar A, Zhang R, Newhauser W (2013) Monte Carlo and analytical model predictions of leakage neutron exposures from passively scattered proton therapy. Med Phys 40: 121714.

5. Fowler JF (1975) Dose fractionation schedules--biologic aspects and applications to high LET radiotherapy. J Can Assoc Radiol 26: 40-43.

6. Stannard C, Vernimmen F, Carrara H, Jones D, Fredericks S, et al. (2013) Malignant salivary gland tumours: Can fast neutron therapy results point the way to carbon ion therapy? Radiother Oncol 109: 262-268.

7. Lukina E, Vazhenin AV, Kuznetsova AI, Munasipov ZZ, Mokichev GV, et al. (2010) [Long-term results of combined photon-neutron radiotherapy for malignant salivary gland tumors at the Ural Neutron Therapy Center]. Vopr Onkol 56: 413-416.

8. Duncan W, Orr JA, Arnott SJ, Jack WJ (1987) Neutron therapy for malignant tumours of the salivary glands. A report of the Edinburgh experience. Radiother Oncol 8: 97-104.

9. Ohnishi T, Takahashi A, Ohnishi K (2002) Studies about space radiation promote new fields in radiation biology. J Radiat Res 43 Suppl: S7-12.

10. Vukovic B, Poje M, Varga M, Radolic V, Miklavcic I, et al. (2010) Measurements of neutron radiation in aircraft. Appl Radiat Isot 68: 2398-2402.

11. Ruhm W, Mares V, Pioch C, Simmer G, Weitzenegger E (2009) Continuous measurement of secondary neutrons from cosmic radiation at mountain altitudes and close to the North Pole--a discussion in terms of H*(10). Radiat Prot Dosimetry 136: 256-261.

12. Ruhm W, Mares V, Pioch C, Weitzenegger E, Vockenroth R, et al. (2009) Measurements of secondary neutrons from cosmic radiation with a Bonner sphere spectrometer at 79 degrees N. Radiat Environ Biophys 48: 125-133.

13. Vukovic B, Radolic V, Miklavcic I, Poje M, Varga M, et al. (2007) Cosmic radiation dose in aircraft--a neutron track etch detector. J Environ Radioact 98: 264-273.

14. Heilbronn L, Nakamura T, Iwata Y, Kurosawa T, Iwase H, et al. (2005) Overview of secondary neutron production relevant to shielding in space. Radiat Prot Dosimetry 116: 140-143.

15. Priyadarshi A, Dominguez G, Thiemens MH (2011) Evidence of neutron leakage at the Fukushima nuclear plant from measurements of radioactive 35S in California. Proc Natl Acad Sci U S A 108: 14422-14425.

16. Mothersill C, Seymour C (2003) Radiation-induced bystander effects, carcinogenesis and models. Oncogene 22: 7028-7033.

17. Mothersill C, Seymour C (1997) Medium from irradiated human epithelial cells but not human fibroblasts reduces the clonogenic survival of unirradiated cells. Int J Radiat Biol 71: 421-427.

18. Dale WM (1940) The effect of X-rays on enzymes. Biochem J 34: 1367-1373.

19. Dale WM (1942) The effect of X-rays on the conjugated protein d-amino-acid oxidase. Biochem J 36: 80-85.

20. Hei TK, Zhou H, Ivanov VN, Hong M, Lieberman HB, et al. (2008) Mechanism of radiation-induced bystander effects: a unifying model. J Pharm Pharmacol 60: 943-950.

21. Sowa Resat MB, Morgan WF (2004) Radiation-induced genomic instability: a role for secreted soluble factors in communicating the radiation response to non-irradiated cells. J Cell Biochem 92: 1013-1019.

22. Asur RS, Thomas RA, Tucker JD (2009) Chemical induction of the bystander effect in normal human lymphoblastoid cells. Mutat Res 676: 11-16.

23. Maguire P, Mothersill C, Seymour C, Lyng FM (2005) Medium from irradiated cells induces dose-dependent mitochondrial changes and BCL2 responses in unirradiated human keratinocytes. Radiat Res 163: 384-390.

24. Rajendran S, Harrison SH, Thomas RA, Tucker JD (2011) The role of mitochondria in the radiation-induced bystander effect in human lymphoblastoid cells. Radiat Res 175: 159-171.

25. Wang H, Yu KN, Hou J, Liu Q, Han W (2013) Radiation-induced bystander effect: Early process and rapid assessment. Cancer Lett, pii: S0304-3835(13)00700-3 doi: 101016/jcanlet201309031.

26. Sokolov MV, Neumann RD (2010) Radiation-induced bystander effects in cultured human stem cells. PLoS One 5: e14195.

27. Shao C, Aoki M, Furusawa Y (2004) Bystander effect in lymphoma cells vicinal to irradiated neoplastic epithelial cells: nitric oxide is involved. J Radiat Res 45: 97-103.

28. Morgan WF, Sowa MB (2007) Non-targeted bystander effects induced by ionizing radiation. Mutat Res 616: 159-164.

29. Liu Z, Mothersill CE, McNeill FE, Lyng FM, Byun SH, et al. (2006) A dose threshold for a medium transfer bystander effect for a human skin cell line. Radiat Res 166: 19-23.

30. Brooks AL (2004) Evidence for 'bystander effects' in vivo. Hum Exp Toxicol 23: 67-70.

31. Belloni P, Latini P, Palitti F (2011) Radiation-induced bystander effect in healthy G(o) human lymphocytes: biological and clinical significance. Mutat Res 713: 32-38.

32. Azzam EI, Little JB (2004) The radiation-induced bystander effect: evidence and significance. Hum Exp Toxicol 23: 61-65.

33. Liu Z, Prestwich WV, Stewart RD, Byun SH, Mothersill CE, et al. (2007) Effective target size for the induction of bystander effects in medium transfer experiments. Radiat Res 168: 627-630.

34. Mothersill C, Smith RW, Fazzari J, McNeill F, Prestwich W, et al. (2012) Evidence for a physical component to the radiation-induced bystander effect? Int J Radiat Biol 88: 583-591.

35. Mothersill C, Smith RW, Heier LS, Teien HC, Land OC, et al. (2013) Radiation-induced bystander effects in the Atlantic salmon (salmo salar L.) following mixed

exposure to copper and aluminum combined with low-dose gamma radiation. Radiat Environ Biophys.

36. Mothersill C, Seymour C (2013) Implications for human and environmental health of low doses of ionising radiation. J Environ Radioact.

37. Edwards GO, Botchway SW, Hirst G, Wharton CW, Chipman JK, et al. (2004) Gap junction communication dynamics and bystander effects from ultrasoft X-rays. Br J Cancer 90: 1450-1456.

38. Hamada N, Maeda M, Otsuka K, Tomita M (2011) Signaling pathways underpinning the manifestations of ionizing radiation-induced bystander effects. Curr Mol Pharmacol 4: 79-95.

39. Ivanov VN, Zhou H, Ghandhi SA, Karasic TB, Yaghoubian B, et al. (2010) Radiation-induced bystander signaling pathways in human fibroblasts: a role for interleukin-33 in the signal transmission. Cell Signal 22: 1076-1087.

40. Chen S, Zhao Y, Han W, Chiu SK, Zhu L, et al. (2011) Rescue effects in radiobiology: unirradiated bystander cells assist irradiated cells through intercellular signal feedback. Mutat Res 706: 59-64.

41. Poon RC, Agnihotri N, Seymour C, Mothersill C (2007) Bystander effects of ionizing radiation can be modulated by signaling amines. Environ Res 105: 200-211.

42. Zhou H, Ivanov VN, Gillespie J, Geard CR, Amundson SA, et al. (2005) Mechanism of radiation-induced bystander effect: role of the cyclooxygenase-2 signaling pathway. Proc Natl Acad Sci U S A 102: 14641-14646.

43. Lyng FM, Maguire P, McClean B, Seymour C, Mothersill C (2006) The involvement of calcium and MAP kinase signaling pathways in the production of radiation-induced bystander effects. Radiat Res 165: 400-409.

44. Baskar R (2010) Emerging role of radiation induced bystander effects: Cell communications and carcinogenesis. Genome Integr 1: 13.

45. Mothersill C, Bristow RG, Harding SM, Smith RW, Mersov A, et al. (2011) A role for p53 in the response of bystander cells to receipt of medium borne signals from irradiated cells. Int J Radiat Biol 87: 1120-1125.

46. Kalanxhi E, Dahle J (2012) The role of serotonin and p53 status in the radiation-induced bystander effect. Int J Radiat Biol 88: 773-776.

47. Ghandhi SA, Yaghoubian B, Amundson SA (2008) Global gene expression analyses of bystander and alpha particle irradiated normal human lung fibroblasts: synchronous and differential responses. BMC Med Genomics 1: 63.

48. Burdak-Rothkamm S, Rothkamm K, Prise KM (2008) ATM acts downstream of ATR in the DNA damage response signaling of bystander cells. Cancer Res 68: 7059-7065.

49. Mothersill C, Saroya R, Smith RW, Singh H, Seymour CB (2010) Serum serotonin levels determine the magnitude and type of bystander effects in medium transfer experiments. Radiat Res 174: 119-123.

50. Mothersill C, Antonelli F, Dahle J, Dini V, Hegyesi H, et al. (2012) A laboratory inter-comparison of the importance of serum serotonin levels in the measurement of a range of radiation-induced bystander effects: overview of study and results presentation. Int J Radiat Biol 88: 763-769.

51. Pinho C, Wong R, Sur RK, Hayward JE, Farrell TJ, et al. (2012) The involvement of serum serotonin levels producing radiation-induced bystander effects for an in vivo assay with fractionated high dose-rate (HDR) brachytherapy. Int J Radiat Biol 88: 791-797.

52. Chapman KL, Al-Mayah AH, Bowler DA, Irons SL, Kadhim MA (2012) No influence of serotonin levels in foetal bovine sera on radiation-induced bystander effects and genomic instability. Int J Radiat Biol 88: 781-785.

53. Chiba S, Saito A, Ogawa S, Takeuchi K, Kumano K, et al. (2002) Transplantation for accidental acute high-dose total body neutron- and gamma-radiation exposure. Bone Marrow Transplant 29: 935-939.

54. Geard CR, Jenkins-Baker G, Marino SA, Ponnaiya B (2002) Novel approaches with track segment alpha particles and cell co-cultures in studies of bystander effects. Radiat Prot Dosimetry 99: 233-236.

55. Nagasawa H, Little JB (1992) Induction of sister chromatid exchanges by extremely low doses of alpha-particles. Cancer Res 52: 6394-6396.

56. Wang C, Smith RW, Duhig J, Prestwich WV, Byun SH, et al. (2011) Neutrons do not produce a bystander effect in zebrafish irradiated in vivo. Int J Radiat Biol 87: 964-973.

57. Kinashi Y, Masunaga S, Nagata K, Suzuki M, Takahashi S, et al. (2007) A bystander effect observed in boron neutron capture therapy: a study of the induction of mutations in the HPRT locus. Int J Radiat Oncol Biol Phys 68: 508-514.

58. Schettino G, Folkard M, Michael BD, Prise KM (2005) Low-dose binary behavior of bystander cell killing after microbeam irradiation of a single cell with focused c(k) x rays. Radiat Res 163: 332-336.

59. Watson GE, Lorimore SA, Macdonald DA, Wright EG (2000) Chromosomal instability in unirradiated cells induced in vivo by a bystander effect of ionizing radiation. Cancer Res 60: 5608-5611.

60. Joiner MC, Van_der_Kogel A (2009) Basic Clinical Radiobiology. London, UK: Macmillan Publishing Solutions.

61. Schwartz JL (2007) Variability: the common factor linking low dose-induced genomic instability, adaptation and bystander effects. Mutat Res 616: 196-200.

62. Morgan WF, Sowa MB (2013) Non-targeted effects induced by ionizing radiation: Mechanisms and potential impact on radiation induced health effects. Cancer Lett pii: S0304-3835(13)00662-9 doi: 101016/jcanlet201309009.

63. Lennox AJ High-Energy Neutron Therapy for Radioresistant Cancers. International Conference on Advanced Neutron Sources – XVIII. Dongguan, Guangdong, China.

64. Chen S, Zhao Y, Zhao G, Han W, Bao L, et al. (2009) Up-regulation of ROS by mitochondria-dependent bystander signaling contributes to genotoxicity of bystander effects. Mutat Res 666: 68-73.

65. Hu B, Wu L, Han W, Zhang L, Chen S, et al. (2006) The time and spatial effects of bystander response in mammalian cells induced by low dose radiation. Carcinogenesis 27: 245-251.

66. Scott AH (2013) The DMSO Handbook for Doctors. Bloomington, Indiana: iUniverse.

67. Han W, Wu L, Hu B, Zhang L, Chen S, et al. (2007) The early and initiation processes of radiation-induced bystander effects involved in the induction of DNA double strand breaks in non-irradiated cultures. Br J Radiol 80 Spec No 1: S7-12.

68. Belyakov OV, Malcolmson AM, Folkard M, Prise KM, Michael BD (2001) Direct evidence for a bystander effect of ionizing radiation in primary human fibroblasts. Br J Cancer 84: 674-679.

69. Prise KM, O'Sullivan JM (2009) Radiation-induced bystander signalling in cancer therapy. Nat Rev Cancer 9: 351-360.

70. Fenech M, Kirsch-Volders M, Natarajan AT, Surralles J, Crott JW, et al. (2011) Molecular mechanisms of micronucleus, nucleoplasmic bridge and nuclear bud formation in mammalian and human cells. Mutagenesis 26: 125-132.

71. Yang M, Kim JS, Son Y, Kim J, Kim JY, et al. (2011) Detrimental effect of fast neutrons on cultured immature rat hippocampal cells: relative biological effectiveness of in vitro cell death indices. Radiat Res 176: 303-310.

72. Dagrosa MA, Crivello M, Perona M, Thorp S, Santa Cruz GA, et al. (2011) First evaluation of the biologic effectiveness factors of boron neutron capture therapy (BNCT) in a human colon carcinoma cell line. Int J Radiat Oncol Biol Phys 79: 262-268.

73. Carnes BA, Grahn D, Thomson JF (1989) Dose-response modeling of life shortening in a retrospective analysis of the combined data from the JANUS program at Argonne National Laboratory. Radiat Res 119: 39-56.

74. Schmid E, Schlegel D, Guldbakke S, Kapsch RP, Regulla D (2003) RBE of nearly monoenergetic neutrons at energies of 36 keV-14.6 MeV for induction of dicentrics in human lymphocytes. Radiat Environ Biophys 42: 87-94.

75. Eastmond DA, Tucker JD (1989) Identification of aneuploidy-inducing agents using cytokinesis-blocked human lymphocytes and an antikinetochore antibody. Environmental and Molecular Mutagenesis 13: 34-43.

76. Cheong HS, Seth I, Joiner MC, Tucker JD (2013) Relationships among micronuclei, nucleoplasmic bridges and nuclear buds within individual cells in the cytokinesis-block micronucleus assay. Mutagenesis 28: 433-440.

CHAPTER 4

Cytogenetic low-dose hyper-radiosensitivity is observed in human peripheral blood lymphocytes

INTRODUCTION

The shape of radiation dose-response curves at low doses has been debated. One reason for the uncertainty of health risks associated with low-dose exposure is the lack of epidemiological evidence (1). Risk estimates for low doses are predicted from linear extrapolation of the relationship between dose and risks observed at higher doses. Linear-no-threshold (LNT) dose-response models are widely used to assess the risks associated with low-dose exposure (2). According to LNT models, the risks of genetic damage increase linearly with dose without any threshold. Regulatory agencies use LNT models to extrapolate risks to low doses from high doses. However in some systems, there is evidence of non-linearity in the low-dose region that contradicts LNT models.

Low-dose hyper-radiosensitivity (HRS) is the phenomenon wherein, at doses below 0.5 Gy, cells are at higher risk of damage per unit dose than at higher doses (3). Non-linear behavior at low doses has been observed in response to different radiation types, certain drugs (e.g., cisplatin and bleomycin) and glutathione S-transferase inhibitors (reviewed in (4)). HRS has been observed in vivo and in many mammalian cell lines (3, 5). Most in vitro studies measured HRS using clonogenic cell-survival assays (6, 7). Failure to observe hypersensitivity in some cell lines may be due to variation in the cell cycle position of the irradiated cells, or to the failure of the underlying molecular pathways (8).

The phenomenon of HRS has been predominantly observed when cells are irradiated in G2 but not in G1 or S (8). Enrichment of MR4 and V79 cells in G1 abolished the elevated levels of cell killing otherwise observed at low doses. This observation demonstrates that enhanced sensitivity of cells irradiated in G2 results from failure of ATM-dependent DNA repair which normally arrests progression of damaged cells into mitosis (9). Low-dose hyper-radiosensitivity has been associated with abrogation of the G2/M checkpoint in rat fibroblasts (10). There is also evidence that hydroxyl radicals are involved in HRS (11). Marples et al. (12) found that HRS was eliminated in V79 cells that were primed with hydrogen peroxide. HRS was first deduced in mouse models of skin and renal damage in vivo (13, 14) and then observed in V79 cells acutely irradiated with single doses of X-rays (3). HRS has since been seen in many mammalian cell lines in response to photons (7, 15) and for different radiation types (X-rays and negative pi-mesons) and biological endpoints (16-19). Until now no study has validated the existence of HRS in human peripheral blood lymphocytes in G2 using structural chromosomal aberrations as the endpoint.

Here we provide the first cytogenetic evidence of low-dose hyper-radiosensitivity in cobalt-60-irradiated human peripheral blood lymphocytes from two healthy adults. This is the first time that the shape of the dose response in G2 has been characterized using structural chromosomal aberrations at such low doses of radiation. HRS may have implications in risk analysis because deviation from LNT models may necessitate re-evaluation of radiation protection standards. The biological effects of low-dose radiation and risks associated with these effects should also be considered while conducting diagnostic and therapeutic treatments involving radiation.

MATERIALS AND METHODS

Subject recruitment, blood collection, and cell culture

Approval from the Wayne State University Human Investigation Committee (HIC) was obtained prior to the recruitment of two healthy female adult blood donors aged 25 and 26. Neither donor had ever undergone chemo- or radiation-therapy. Peripheral blood (50 mL) from each donor was drawn into Vacutainer Sodium Heparin tubes (Becton Dickinson). Immediately following phlebotomy, blood from each donor was aliquoted into tissue culture flasks (26 flasks each for G0 and G2 exposures). Blood (800 µL) was placed into non-vented T25 flasks (Corning, NY and ISC BioExpress, Kaysville, UT) containing 10 mL of medium consisting of RPMI1640 (GIBCO, Grand Island, NY or Hyclone, Logan, UT) supplemented with 15% fetal bovine serum (Atlanta Biologicals, Lawrenceville, GA), 2% phytohemagglutinin (Gibco), 1% penicillin–streptomycin (100 units/ml penicillin G Sodium, 100 µg/ml streptomycin sulfate in 0.85% saline; GIBCO, Grand Island, NY) and 2 mM L-glutamine (GIBCO, Grand Island, NY). The media was pre-warmed to 37°C prior to the addition of the blood. Culture flasks caps were kept loose, and tightened only when being transported and irradiated.

Irradiation, slide preparation and staining

All irradiations were performed at the Gershenson Radiation Oncology Center, Wayne State University with a Cobalt-60 source in a Theratron 780 radiotherapy unit (MDS Nordion, Canada), at a dose rate of 0.25 Gy/min. The samples were transported to and from the cytogenetics laboratory (a 5 minute drive) in an insulated container with warm packs at 37°C. Cells were acutely irradiated at doses of 0, 0.1, 0.2, 0.3, 0.4, 0.5,

0.6, 0.7, 0.8, 0.9, 1.0, 1.25 and 1.5 Gy. The 0 Gy (control) was sham-irradiated. Careful consideration was given to the temperature of the cells before, during and after radiation. During radiation the flasks were in a room where the ambient temperature was approximately 25°C, without warm packs. The flasks that were in this temperature for the longest duration were those irradiated with 1.5 Gy, which required an exposure time of 6 minutes. For both G0 and G2 exposures, blood was immediately placed into culture after the blood draw. For G0 exposures the cells were irradiated immediately and Colcemid (KaryoMAX, Gibco) was added 44 hours later at a final concentration of 0.1 μg/mL. For G2 exposures, blood was irradiated after 46 hours in culture and Colcemid was added immediately afterwards. After radiation all flasks were placed upright in a fully humidified incubator with 5% CO_2 at 37°C. For G0 and G2 exposures cells were harvested four and two hours after the addition of Colcemid, respectively, i.e. 48 hours after culture initiation. Slides of cells in metaphase were prepared and block-stained with Giemsa using standard techniques.

Scoring of structural chromosomal aberrations

All slides were coded prior to scoring to prevent observer bias. All scoring was performed on a Nikon Eclipse E200 microscope at 1000X total magnification. One well-trained slide reader scored at least 200 cells in metaphase for each treatment condition. Cells were scored for structural chromosomal aberrations including chromatid and chromosome breaks, and chromatid and chromosome exchanges. Gaps were also recorded but were not included in the final data analyses. The term “total aberrations” refers to the sum of all the different kinds of chromosomal damage including chromatid

and chromosome damage for each cell cycle phase, and “total abnormal cells” refers to the number of cells that had any kind of chromosomal damage.

Statistical Analyses

Linear and non-linear regressions were performed using JMP software (version 6.0, SAS Institute, Inc.) for each aberration type in G2 and G0. Student’s t-test was used to compare the slopes of the regression lines. *P*-values <0.05 were considered statistically significant.

RESULTS

These data provide the first cytogenetic evidence of low-dose radiation hypersensitivity in human cells. For both donors and cell cycle phases, we recorded chromatid and chromosome breaks, and chromatid and chromosome exchanges. The number of cells scored and the frequency of each aberration type for each treatment condition are provided in Tables 4.1 and 4.2 for Donors 1 and 2, respectively. As expected (20), chromatid-type damage was most prevalent in G2 and chromosome-type damage was most prevalent in G0 (Tables 4.1 and 4.2); for this reason Tables 4.3 and 4.4 report only the most prevalent aberration types associated with each cell cycle phase. For both donors and cell cycle phases, the frequencies of all aberrations considered together and the associated regression fits are shown in Figure 4.1 and 4.2.

Summaries of the regression analyses and ratios of the slopes of the low-dose to high-dose regions for both donors for G2 and G0 are shown in Tables 4.3 and 4.4, respectively. Doses ≤0.4 Gy were considered as the low-dose region, while doses ≥0.5 Gy were considered as the high-dose region; the 0 Gy (control) group was included in all regression analyses. The highest doses included in the analyses were 1.25 Gy and 1 Gy for Donors 1 and 2, respectively; doses above these values were excluded to avoid poor regression fits due to the decline in the frequencies of aberrations at these high doses for cells irradiated in G2 (Figure 4.1 A and 4.2 A), which are likely due to greater cell cycle delay of the most heavily damaged cells.

Table 4.1. Donor 1 data by dose and aberration type for G2 and G0 phases.

Dose (in Gy)	Number of cells scored	All aberrations / 100 cells	Total number of abnormal cells/ 100 cells	Chromatid breaks/ 100 cells	Chromatid exchanges / 100 cells	Chrom-osome breaks/ 100 cells	Chrom-osome exchanges /100 cells
Donor 1, G2							
0	200	1.5	1.5	0	0	1.0	0.5
0.1	200	7.0	6.0	1.0	1.0	2.0	3.0
0.2	200	34.0	28.0	25.5	2.0	2.5	4.0
0.3	201	33.8	26.4	13.9	8.0	4.5	7.5
0.4	202	49.0	29.7	23.3	8.4	11.4	5.9
0.5	201	34.3	22.9	22.9	7.0	2.5	2.0
0.6	200	42.0	26.0	22.5	7.0	2.5	10.0
0.7	207	60.4	30.9	47.3	6.8	2.4	3.9
0.8	200	63.0	36.5	32.5	10.5	2.5	17.5
0.9	200	114.0	53.5	92.5	16.0	2.5	3.0
1	200	93.0	43.5	68.5	14.5	2.0	8.0
1.25	204	149.0	55.4	108.8	24.5	5.4	10.3
1.5	200	107.0	39.5	72.5	19.0	5.0	10.5
Donor 1, G0							
0	201	0	0	0	0	0	0
0.1	200	0.5	0.5	0	0	0.5	0
0.2	201	0.5	0.5	0	0	0.5	0
0.3	200	3.5	2.0	1.0	0	1.0	1.5
0.4	200	2.5	2.0	0	0	1.5	1.0
0.5	200	7.5	5.0	0	0	4.0	3.5
0.6	200	9.5	7.5	0	0.5	5.0	4.0
0.7	203	13.8	9.9	1.5	0	7.9	4.4
0.8	200	9.0	5.5	0.5	0	4.5	4.0
0.9	200	11.5	9.0	0	0	6.0	5.5
1	200	13.0	8.0	0.5	0	9.0	3.5
1.25	200	18.0	12.5	0	0	10.5	7.5
1.5	200	24.0	16.0	0	0	14.0	10.0

Table 4.2. Donor 2 data by dose and aberration type for G2 and G0 phases.

Dose (in Gy)	Number of cells scored	All aberrations / 100 cells	Total number of abnormal cells/ 100 cells	Chromatid breaks/ 100 cells	Chromatid exchanges / 100 cells	Chrom-osome breaks/ 100 cells	Chrom-osome exchanges / 100 cells
Donor 2, G2							
0	200	0	0	0	0	0	0
0.1	205	12.2	9.8	11.2	0.5	0	0.5
0.2	200	16.5	12.5	15.5	1.0	0	0
0.3	201	24.9	12.9	20.9	3.0	0	1.0
0.4	200	31.0	23.5	24.0	7.0	0	0
0.5	201	23.9	16.4	17.9	5.5	0.5	0
0.6	200	32.5	21.5	28.0	4.0	0	0.5
0.7	200	37.5	23.0	28.5	9.0	0	0
0.8	200	64.5	30.5	56.5	7.5	0	0.5
0.9	200	74.0	34.5	63.0	9.5	0	1.5
1	200	72.0	35.5	61.5	10.0	0.5	0
1.25	201	48.3	23.4	39.3	8.5	0	0.5
1.5	200	40.5	24.0	31.0	9.5	0	0
Donor 2, G0							
0	200	2.5	2.0	0	0	2.0	0.5
0.1	200	1.0	1.0	0	0	1.0	0
0.2	200	3.0	2.5	0	0	2.0	1.0
0.3	200	2.5	2.5	0	0	1.5	1.0
0.4	200	1.0	1.0	0	0	0.5	0.5
0.5	201	4.0	3.5	0	0	1.5	2.5
0.6	200	3.0	2.0	0	0	1.5	1.5
0.7	200	3.5	3.0	0	0	2.0	1.5
0.8	200	6.5	4.5	0	0	3.0	3.5
0.9	203	10.8	8.4	0	0	6.9	3.9
1	200	6.5	6.5	0	0	2.5	4.0
1.25	201	11.9	9.5	0	0	8.0	4.0
1.5	200	20.5	16.0	0.5	0	14.5	5.5

Table 4.3. G2 regression analyses and ratios of slopes.

Aberration type/100 metaphases	Slope (linear coefficient ± S.E)		Ratio of slopes	p- value
	Low-dose* Linear fit	High-dose† Linear-quadratic fit		
Donor 1				
All aberrations	121.85 ± 20.56	38.25 ± 40.63	3.2	0.006
Abnormal cells	76.77 ± 21.08	48.36 ± 16.70	1.6	0.08
Chromatid breaks	59.47 ± 27.17	21.14 ± 49.97	2.8	0.14
Chromatid exchanges	23.80 ± 4.99	3.70 ± 5.52	6.4	0.003
Average			3.5 ± 1.02	
Donor 2				
All aberrations	74.70 ± 6.48	25.05 ± 31.45	3.0	0.003
Abnormal cells	50.18 ± 10.04	32.02 ± 6.86	1.6	0.026
Chromatid breaks	57.68 ± 8.23	14.97 ± 32.14	3.9	0.009
Chromatid exchanges	16.50 ± 4.32	9.64 ± 5.69	1.7	0.084
Average			2.5 ± 0.55	

* 0 to 0.4 Gy

† 0, and 0.5 Gy-1.25 Gy for Donor 1; 0, and 0.5-1.0 Gy for Donor 2.

Table 4.4. G0 regression analyses and ratios of slopes.

Aberration type/100 metaphases	Slope (linear coefficient ± S.E)				Ratio of slopes	p-value
	Low-dose*	Type of fit (L, LQ)†	High-dose‡	Type of fit (L, LQ)†		
Donor 1						
All aberrations	8.00 ± 3.05	L	13.28 ± 2.01	L	0.60	0.18
Abnormal cells	5.50 ± 1.26	L	11.16 ± 5.78	LQ	0.49	0.03
Chromosome breaks	3.50 ± 0.50	L	7.56 ± 4.48	LQ	0.46	0.02
Chromosome exchanges	3.50 ± 1.60	L	5.75 ± 3.23	LQ	0.61	0.27
Average					0.54 ± 0.03	
Donor 2						
All aberrations	-1.50 ± 3.30	L	6.13 ± 2.86	L	-0.24	0.06
Abnormal cells	-0.50 ± 2.75	L	5.30 ± 2.20	L	-0.09	0.07
Chromosome breaks	-2.50 ± 1.89	L	2.57 ± 2.29	L	-0.97	0.06
Chromosome exchanges	1.00 ± 1.41	L	0.64 ± 3.05	LQ	1.56	0.42
Average					0.06 ± 0.53	

* 0 to 0.4 Gy

† L= Linear, LQ= Linear-quadratic

‡ 0, and 0.5 Gy-1.25 Gy for Donor 1; 0, and 0.5-1.0 Gy for Donor 2.

For G2, the low-dose region slopes were calculated using a linear regression model, while the slopes of the high-dose regions were calculated using a linear-quadratic model, in accordance with conventional radiation dosimetry models (21). For Donor 1, for all aberrations and chromatid exchanges, the low-dose region slopes were significantly steeper ($p<0.05$) than the linear term of the linear-quadratic model of the high-dose region (Table 4.3). For Donor 2 every aberration type exhibited a steeper slope at the low doses ($p<0.05$) (Table 4.3). The average of the ratios of the low-dose region slopes to the high-dose region slopes was 3.50±1.02 (mean±S.E.) and 2.50±0.55, for Donors 1 and 2, respectively (Table 4.3); these ratios were not significantly different (t-test, $p>0.05$).

No low-dose radiation hypersensitivity was observed in G0 for either donor (Table 4.4). For Donor 1 cells irradiated in G0, all the low-dose region slopes were calculated using a linear regression model and all the high-dose region slopes except for all aberrations considered together were calculated using a linear-quadratic model. The decision whether to use a linear or a linear-quadratic model was based on whichever model gave the best fit and made the most biological sense (21). For Donor 2 cells irradiated in G0, all the low-dose and high-dose region slopes were calculated using a linear model except that the high-dose region slope for chromosome exchanges was calculated using a linear-quadratic model. Linear fits were chosen over linear-quadratic fits for high-doses in G0 for Donor 2 because linear-quadratic fits either gave negative linear or negative dose-squared coefficients. Low-dose hyper-radiosensitivity was not observed in G0 for either donor, i.e. the slope of the low-dose region was not higher than the slope obtained by back-extrapolating from the high-dose region. The

average of the ratios of low-dose region slopes to the high-dose region slopes was 0.54±0.03 for Donor 1 and 0.06±0.53 (mean±S.E.) for Donor 2 (Table 4.4); these ratios were not significantly different (t-test, $p>0.05$).

The most reasonable way to compare the amounts of chromosome damage in both cell cycle phases is to evaluate the frequencies of all aberration types considered together, because as noted above, the types of damage differ in G0 and G2. Figure 4.1 B and 4.2 B show the regression fits for all aberrations considered together for donors 1 and 2, respectively, for G2 and G0 exposures. For cells irradiated in G2, the slope of the low-dose region is approximately 3 times steeper ($p<0.01$) than that obtained by back-extrapolation from high doses (Figure 4.1 A, 4.2 A, Table 4.3), indicating low-dose hyper-radiosensitivity. For cells irradiated in G0, the slope of low-dose region is not steeper than the high-dose region slope for either donor (Figure 4.1 B and 4.2 B), indicating an absence of low-dose hyper-radiosensitivity.

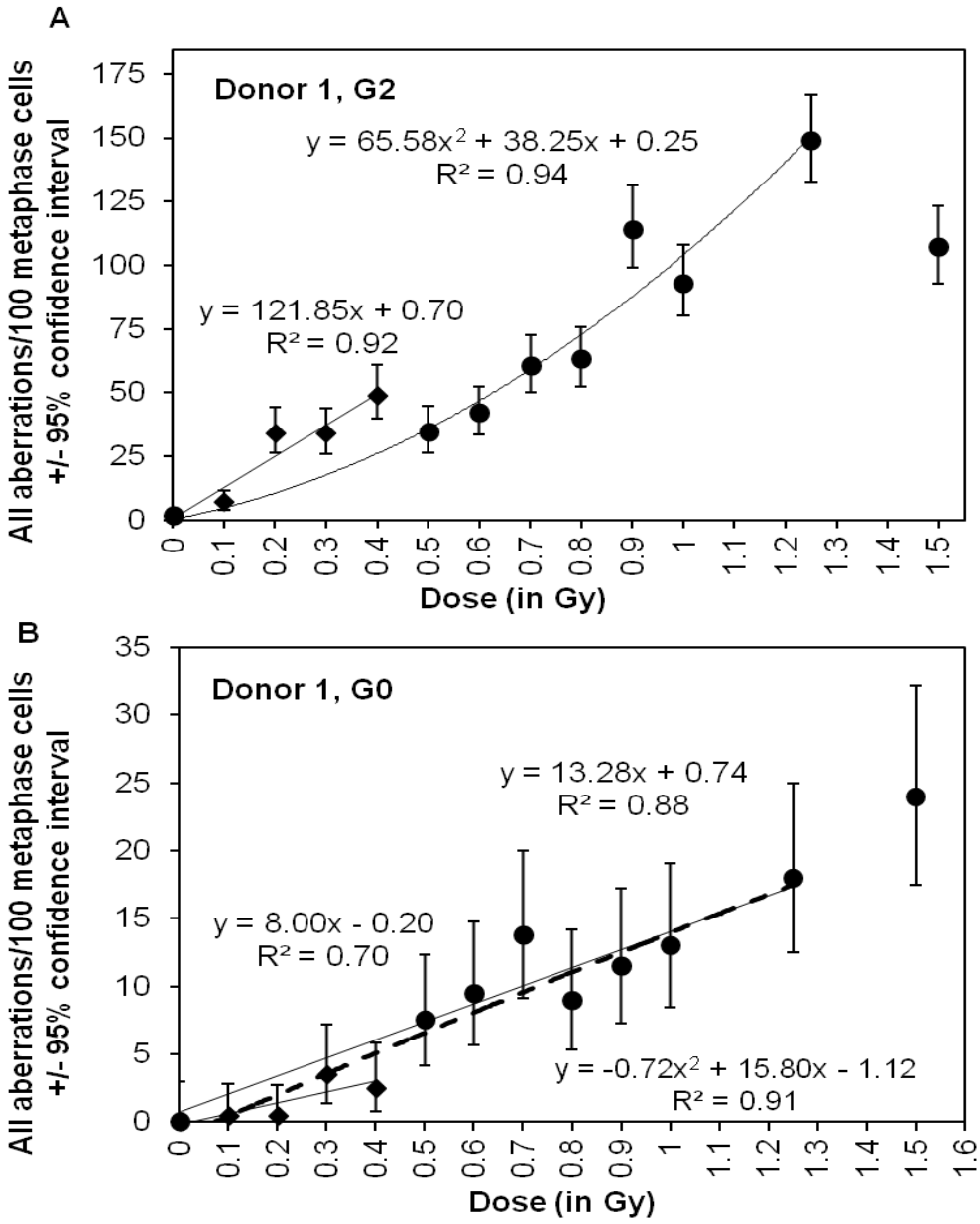

Figure 4.1 Upper panel: Donor 1 cells irradiated in G2, where the slopes of the low- and high-dose regions were fitted to linear and linear-quadratic models, respectively. Cells show hyper-radiosensitivity up to 0.4 Gy. The low-dose region slope is higher than that obtained by back-extrapolation of the high-dose region slope, indicating low-dose hyper-radiosensitivity. Lower panel: Donor 1 G0 slopes of the low- and high-dose regions fitted to linear models, for all aberration types considered all together. No low dose hyper-radiosensitivity was observed in G0. The dashed line in panel B is for both low-and high-dose data together fitted with a linear-quadratic model.

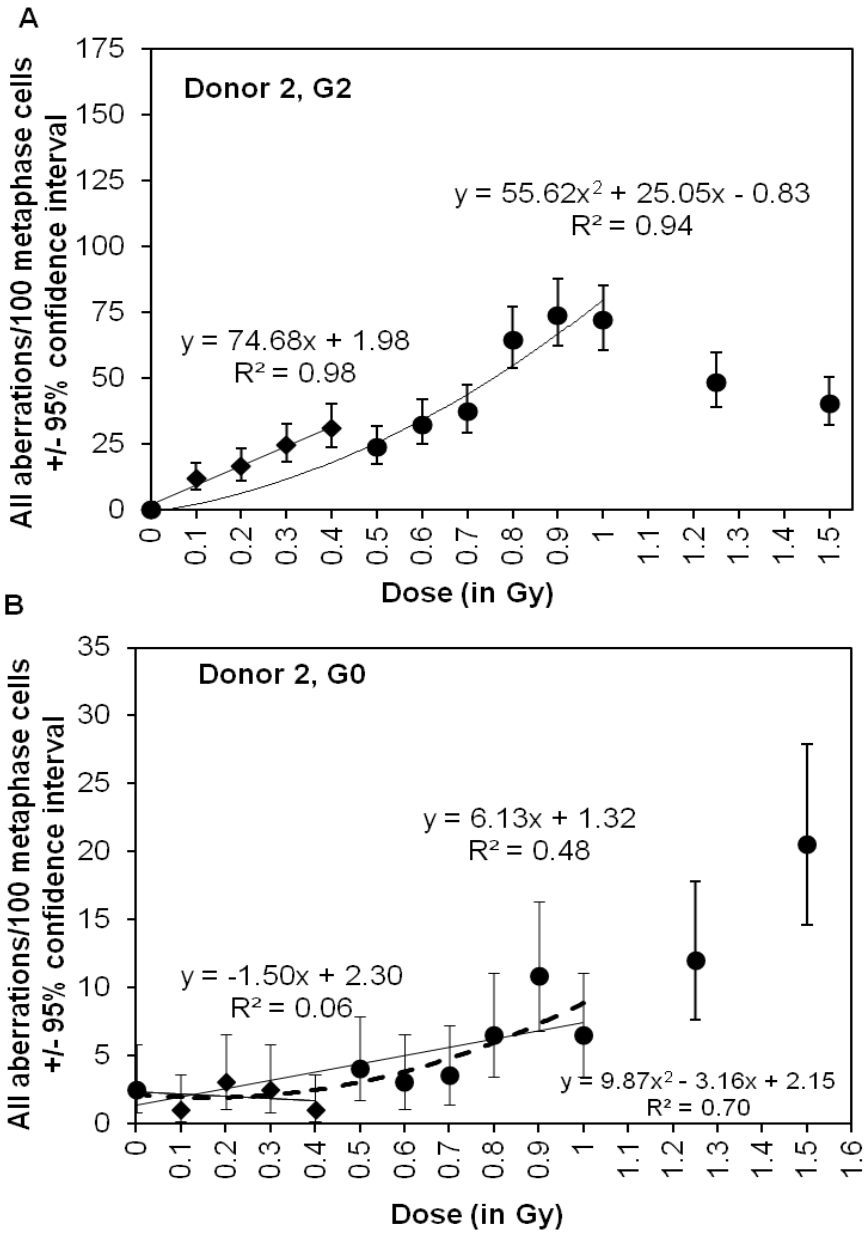

Figure 4.2 Upper panel: Donor 2 cells irradiated in G2, where the slopes of the low- and high-dose regions were fitted to linear and linear-quadratic models, respectively. Cells show hyper-radiosensitivity up to 0.4 Gy. The low-dose region slope is higher than that obtained by back-extrapolation of the high-dose region slope, indicating low-dose hyper-radiosensitivity. Lower panel: Donor 2 G0 slopes of the low- and high-dose regions fitted to linear models, for all aberration types considered all together. No low dose hyper-radiosensitivity was observed in G0. The dashed line in panel B is for both low-and high-dose data together fitted with a linear-quadratic model.

Radiation sensitivity, i.e. the cytogenetic effect per unit dose, is illustrated in Figure 4.3 for each donor and cell cycle phase. Here, the same data as shown in Figure 4.1 and 4.2 are re-plotted such that the vertical axis is the frequency of aberrations per unit dose, i.e. the slope of the line from the 0-dose value to each individual data point. For both donors, there is evidence of hypersensitivity in G2 at doses ≤0.4 Gy compared to doses ≥0.5 Gy. No low-dose hyper-radiosensitivity was observed in G0. Compared to Donor 1, Donor 2 showed a more consistent pattern of hyper-radiosensitivity. For Donor 2, the effect per unit dose for all doses ≤0.4 Gy was high with cells being most radiosensitive at 0.1 Gy. However, for Donor 1, the 0.1 Gy dose had low radio-sensitivity, and doses 0.2-0.4 Gy showed sensitivity higher than 0.1 Gy.

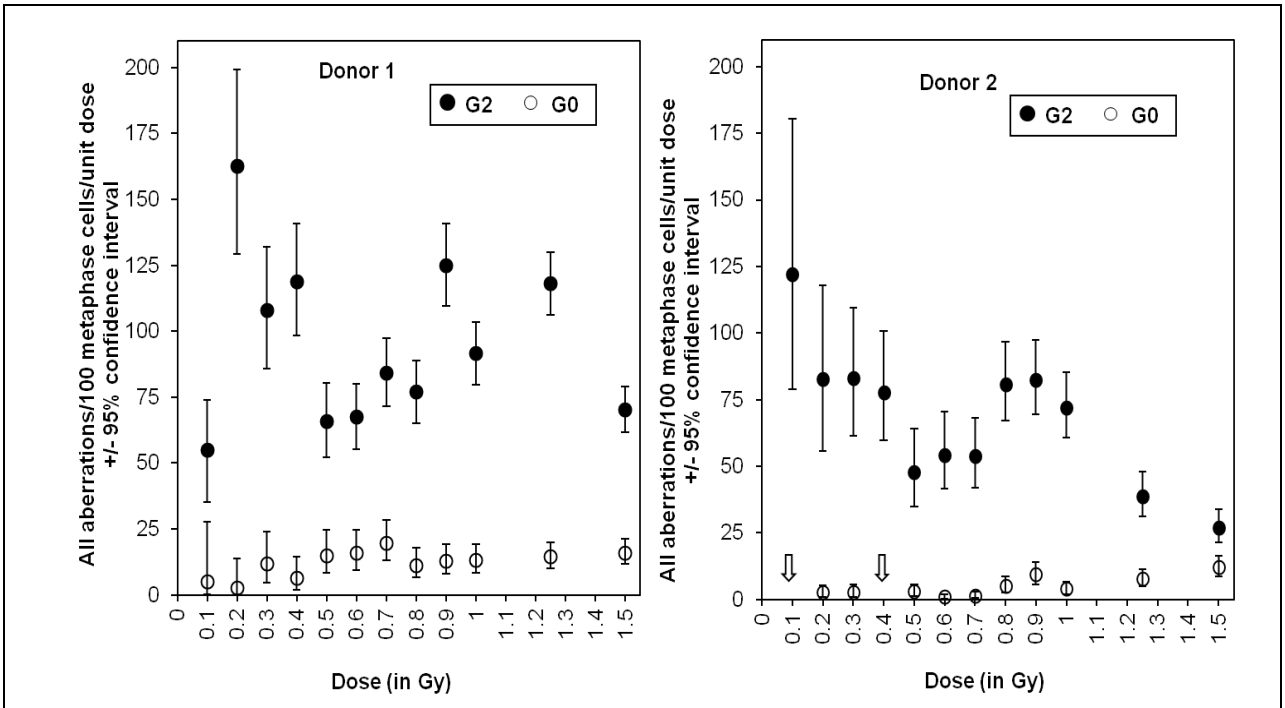

Figure 4.3 Radiation sensitivity of cells irradiated in G2 compared to cells irradiated in G0 for all aberration types considered together. Cells irradiated in G2 clearly show more hypersensitivity than cells irradiated in G0. For Donor 2, G0 phase, the values for 0.1 and 0.4 Gy were negative and are not shown (indicated by arrows).

DISCUSSION

The goal of the work described here was to characterize the shape of the cytogenetic dose-response curve for low doses of cobalt-60 gamma rays without any prejudice towards the direction of any non-linearity that might be observed. Our data provide the first cytogenetic evidence of low-dose radiation hypersensitivity in human peripheral blood lymphocytes in response to cobalt-60 gamma rays. The spectrum of chromosomal aberrations observed in G2 and G0 is in accordance with the classical theory of aberration formation where chromosome-type aberrations are induced in cells irradiated in G0 and chromatid-type aberrations are observed G2 (20). We did observe low levels of chromosome-type damage in G2-irradiated cells which are likely due to the presence of a few cells that were in S-phase at the time of exposure. We also observed small amounts of chromatid-type damage in G0-irradiated cells, which appear to be spontaneous and not radiation-induced. These latter aberrations may be due to endogenous reactive oxygen species (ROS) which have been reported to play a role in inducing chromatid-type aberrations in G0-irradiated cells (22).

For G2-irradiated cells, both donors show hyper-radiosensitivity at low doses. There is variability in the radiation responses between the two donors which may be attributable to genetic differences. For both donors, the low-dose region slope is three times steeper ($p<0.01$) than the slope obtained by back-extrapolation from high doses, clearly providing evidence of cytogenetic low-dose hyper-radiosensitivity. Our results are in agreement with the low-dose hyper-radiosensitivity that has been previously shown to occur for cell killing in vitro and in vivo in different cell systems including normal and tumor cells (3, 23, 24), and subsequently reviewed in (6). In the present

study the hyper-radiosensitivity peak was observed at 0.1 and 0.2 Gy for Donors 2 and 1, respectively. The aberration frequencies when considered together were fairly constant over the dose range 0.2-0.5 Gy which may be due to induction of DNA repair mechanisms (7). The full spectrum of chromosomal aberrations was analyzed here, which may provide insight to the underlying mechanisms of low-dose hyper-radiosensitivity. The presence of chromatid breaks with the highest damage per unit dose at doses up to 0.4 Gy suggests that at least some cells damaged by these low doses were able to enter mitosis without these breaks being repaired. The peak dose for hyper-radiosensitivity differs and may depend on the cell type, endpoint being evaluated and radiation type. The underlying mechanism of low-dose hyper-radiosensitivity as hypothesized originally by Marples et al. (8) is the failure to activate the ATM protein and thus bypass the G2/M checkpoint due to sub-threshold DNA damage induced at these low doses. In another study, radiosensitivity and formation of ROS have been shown to be closely associated following irradiation (25).

For cells irradiated in G0, the slope of the low dose region is not steeper than the high-dose region slope for either donor, indicating an absence of low-dose hyper-radiosensitivity. This suggests that cells have enough time for repair if they are irradiated in G0, because cells are known to be more radioresistant in G0/S compared to G2 (26). Our results are in contrast those of Nasnova et al. (27) who observed hypersensitivity in irradiated G0 lymphocytes at 1-7 cGy. Their conclusions are based on the observation of significant amounts of chromatid-type aberrations in G0. However, they did not provide any conclusive reason for their observations, which are in contrast

to the classical norm (20), and may simply be due to ROS-related baseline DNA damage (22).

Low-dose hyper-radiosensitivity could be exploited clinically if radiotherapy were delivered in a large number of dose fractions, each of which is <0.5 Gy. There is a possibility of taking advantage of the sensitivity of tumor cells at low doses which are otherwise resistant to radiation at higher doses (26). Two studies have reported hyper-radiosensitivity in a tumor model system following fractionated X-irradiation (18, 28). In a cell survival study, human radioresistant T98G glioblastoma cells were found to show marked radiosensitivity to low doses (24). In a related study which also evaluated clonogenic survival, five human radioresistant glioma cell lines demonstrated radiosensitivity (29). Recently, very promising results were obtained in a clinical trial where glioblastoma patients showed a significant increase in overall survival using ultra fractionation protocols (three times daily dose of 0.8 Gy instead of a single large dose of 2 or 2.4 Gy (30). To further identify the clinical potential of using the phenomenon of low-dose hyper-radiosensitivity in radiotherapy, a similar cytogenetic study could be performed on tumor cells to determine whether they exhibit low-dose hyper-radiosensitivity. Information obtained should be relevant to radiation oncologists when administering radiotherapy to cancer patients.

The findings reported here are in accordance with previous in vitro and in vivo cell killing studies (3, 5, 6, 16). As reviewed in (31), the report of the French Academy of Sciences and the French Academy of Medicine also questions the validity of the LNT model. However, our data are in contrast with conclusions made by BEIR VII that supports LNT as an accurate risk model (31).

The extent to which low doses might be harmful to human cells will depend on the type of cells, their sensitivity to radiation, and on the fraction of cells in the most sensitive cell cycle phase. Quantifying the effect that low-dose hyper-radiosensitivity has on the human body may be difficult because of differential sensitivity among cell types, which may be at least partially attributable to differences in the length of their cell cycle phases. The net effect of low-dose hyper-radiosensitivity on cancer risks in cell populations and tissues will depend on whether the increased damage occurring at these low doses, as reported here, increases cytotoxicity and/or the number of survivable mutations. Further work needs to be done to couple mutational assays with the ultimate fate of cells after damage by low doses of radiation.

The work reported here is the first to provide cytogenetic evidence of low-dose hyper-radiosensitivity in human cells using structural chromosomal aberrations. There is a potential of exploiting the phenomenon of low-dose hyper-radiosensitivity in radiotherapy to kill tumor cells that may be otherwise resistant to higher doses. These results indicate that LNT models may not always correctly assess radiation risk the low-dose region.

REFERENCES

1. Little MP, Wakeford R, Tawn EJ*, et al.* Risks associated with low doses and low dose rates of ionizing radiation: why linearity may be (almost) the best we can do. *Radiology* 2009;251:6-12.
2. ICRP. The 2007 Recommendations of the International Commission on Radiological Protection. ICRP publication 103. *Ann ICRP* 2007;37:1-332.
3. Marples B, Joiner MC. The response of Chinese hamster V79 cells to low radiation doses: evidence of enhanced sensitivity of the whole cell population. *Radiat Res* 1993;133:41-51.
4. Skov KA. Radioresponsiveness at low doses: hyper-radiosensitivity and increased radioresistance in mammalian cells. *Mutat Res* 1999;430:241-253.
5. Joiner MC, Marples B, Johns H. The response of tissues to very low doses per fraction: a reflection of induced repair? *Recent Results Cancer Res* 1993;130:27-40.
6. Marples B, Wouters BG, Collis SJ*, et al.* Low-dose hyper-radiosensitivity: a consequence of ineffective cell cycle arrest of radiation-damaged G2-phase cells. *Radiat Res* 2004;161:247-255.
7. Joiner MC, Marples B, Lambin P*, et al.* Low-dose hypersensitivity: current status and possible mechanisms. *Int J Radiat Oncol Biol Phys* 2001;49:379-389.
8. Marples B, Wouters BG, Joiner MC. An association between the radiation-induced arrest of G2-phase cells and low-dose hyper-radiosensitivity: a plausible underlying mechanism? *Radiat Res* 2003;160:38-45.

9. Krueger SA, Joiner MC, Weinfeld M*, et al.* Role of apoptosis in low-dose hyper-radiosensitivity. *Radiat Res* 2007;167:260-267.

10. Krueger SA, Wilson GD, Piasentin E*, et al.* The effects of G2-phase enrichment and checkpoint abrogation on low-dose hyper-radiosensitivity. *Int J Radiat Oncol Biol Phys* 2010;77:1509-1517.

11. Boreham DR, Mitchel RE. DNA lesions that signal the induction of radioresistance and DNA repair in yeast. *Radiat Res* 1991;128:19-28.

12. Marples B, Joiner MC, Skov KA. The effect of oxygen on low-dose hypersensitivity and increased radioresistance in Chinese hamster V79-379A cells. *Radiat Res* 1994;138:S17-20.

13. Joiner MC, Denekamp J. The effect of small radiation doses on mouse skin. *Br J Cancer Suppl* 1986;7:63-66.

14. Joiner MC, Johns H. Renal damage in the mouse: the response to very small doses per fraction. *Radiat Res* 1988;114:385-398.

15. Mothersill C, Seymour CB, Joiner MC. Relationship between radiation-induced low-dose hypersensitivity and the bystander effect. *Radiat Res* 2002;157:526-532.

16. Marples B, Adomat H, Koch CJ*, et al.* Response of V79 cells to low doses of X-rays and negative pi-mesons: clonogenic survival and DNA strand breaks. *Int J Radiat Biol* 1996;70:429-436.

17. Wouters BG, Sy AM, Skarsgard LD. Low-dose hypersensitivity and increased radioresistance in a panel of human tumor cell lines with different radiosensitivity. *Radiat Res* 1996;146:399-413.

18. Dey S, Spring PM, Arnold S*, et al.* Low-dose fractionated radiation potentiates the effects of Paclitaxel in wild-type and mutant p53 head and neck tumor cell lines. *Clin Cancer Res* 2003;9:1557-1565.

19. Short SC, Woodcock M, Marples B*, et al.* Effects of cell cycle phase on low-dose hyper-radiosensitivity. *Int J Radiat Biol* 2003;79:99-105.

20. Savage JR. Classification and relationships of induced chromosomal structual changes. *J Med Genet* 1976;13:103-122.

21. Lee SP, Leu MY, Smathers JB*, et al.* Biologically effective dose distribution based on the linear quadratic model and its clinical relevance. *Int J Radiat Oncol Biol Phys* 1995;33:375-389.

22. Duell T, Lengfelder E, Fink R*, et al.* Effect of activated oxygen species in human lymphocytes. *Mutat Res* 1995;336:29-38.

23. Malaise EP, Lambin P, Joiner MC. Radiosensitivity of human cell lines to small doses. Are there some clinical implications? *Radiat Res* 1994;138:S25-27.

24. Short S, Mayes C, Woodcock M*, et al.* Low dose hypersensitivity in the T98G human glioblastoma cell line. *Int J Radiat Biol* 1999;75:847-855.

25. Ogawa Y, Takahashi T, Kobayashi T*, et al.* Comparison of radiation-induced reactive oxygen species formation in adult articular chondrocytes and that in human peripheral T cells: possible implication in radiosensitivity. *Int J Mol Med* 2003;11:455-459.

26. Joiner MC, Kogel AVd. Basic Clinical Radiobiology. Vol Fourth edition edn (Hodder Arnold). 2009.

27. Nasonova EA, Shmakova NL, Komova OV*, et al.* Cytogenetic effects of low-dose radiation with different LET in human peripheral blood lymphocytes. *Radiat Environ Biophys* 2006;45:307-312.

28. Short SC, Kelly J, Mayes CR*, et al.* Low-dose hypersensitivity after fractionated low-dose irradiation in vitro. *Int J Radiat Biol* 2001;77:655-664.

29. Short SC, Mitchell SA, Boulton P*, et al.* The response of human glioma cell lines to low-dose radiation exposure. *Int J Radiat Biol* 1999;75:1341-1348.

30. Beauchesne P. Three-times daily ultrafractionated radiation therapy, a novel and promising regimen for glioblastoma patients. *Cancers (Basel)* 2013;5:1199-1211.

31. Tubiana M, Aurengo A, Averbeck D*, et al.* Recent reports on the effect of low doses of ionizing radiation and its dose-effect relationship. *Radiat Environ Biophys* 2006;44:245-251.

ABSTRACT

BYSTANDER EFFECTS DUE TO NEUTRONS, AND LOW-DOSE HYPER-RADIOSENSITIVITY TO GAMMA RAYS IN HUMAN CELLS USING CYTOGENETICS

by

ISHEETA SETH

August 2014

Advisor: Dr. James D. Tucker

Major: Biological Science

Degree: Doctor of Philosophy

Chapter 2:

Micronuclei have been used extensively in studies as an easily-evaluated indicator of DNA damage but little is known about their association with other types of damage such as nucleoplasmic bridges and nuclear buds. Radiation-induced clastogenic events were evaluated via the cytokinesis-block micronucleus assay in two normal human lymphoblastoid cell lines exposed to neutrons or gamma radiation. Micronuclei, nucleoplasmic bridges and nuclear buds were enumerated by recording the coincident presence of these endpoints within individual cells, and the associations among these three endpoints were evaluated for all treatment conditions. The common odds ratios for micronuclei and nucleoplasmic bridges were found to be significantly larger than unity, indicating that the presence of one or more micronuclei in a cell imposes a significant risk for having one or more nucleoplasmic bridges in that same

cell, and vice versa. The strength of this association did not change significantly with radiation dose. Common odds ratios for association between micronuclei and buds, and between bridges and buds were also found to be significantly higher than unity. However, associations between micronuclei and buds could not be calculated for some treatments due to heterogeneity in the odds ratios, and hence may depend on radiation dose. This study provides evidence for how paired analyses among genetic endpoints in the cytokinesis-block micronucleus assay can provide information concerning abnormalities of cell division and possibly about structural chromosomal rearrangements induced by radiation.

Chapter 3:

Bystander effects have been observed repeatedly in mammalian cells following photon and alpha particle irradiation. However, few studies have been performed to investigate bystander effects arising from neutron irradiation. Here we asked whether neutrons also induce a bystander effect in two normal human lymphoblastoid cell lines. These cells were exposed to fast neutrons produced by targeting a near-monoenergetic 50.5 MeV proton beam at a Be target (17 MeV average neutron energy), and irradiated-cell conditioned media (ICCM) was transferred to unirradiated cells. The cytokinesis-block micronucleus assay was used to quantify genetic damage in radiation-naïve cells exposed to ICCM from cultures that received 0 (control), 0.5, 1, 1.5, 2, 3 or 4 Gy neutrons. Cells grown in ICCM from irradiated cells showed no significant increase in the frequencies of micronuclei or nucleoplasmic bridges compared to cells grown in ICCM from sham irradiated cells for either cell line. However, the neutron beam has a photon dose-contamination of 5%, which may modulate a neutron-induced bystander

effect. To determine whether these low doses of contaminating photons can induce a bystander effect, cells were irradiated with cobalt-60 at doses equivalent to the percent contamination for each neutron dose. No significant increase in the frequencies of micronuclei or bridges was observed at these doses of photons for either cell line when cultured in ICCM. As expected, high doses of photons induced a clear bystander effect in both cell lines for micronuclei and bridges ($p < 0.0001$). These data indicate that neutrons do not induce a bystander effect in these cells. Finally, neutrons had a relative biological effectiveness of 2.0 ± 0.13 for micronuclei and 5.8 ± 2.9 for bridges compared to cobalt-60. These results may be relevant to radiation therapy with fast neutrons and for regulatory agencies setting standards for neutron radiation protection and safety.

Chapter 4:

The shape of the ionizing radiation response curve at very low doses has been the subject of considerable debate. Linear-no-threshold (LNT) models are widely used to estimate risks associated with low dose exposures. However, the low-dose hyper-radiosensitivity (HRS) phenomenon, in which cells are especially sensitive at low doses but then show increased radioresistance at higher doses, provides evidence of nonlinearity in the low dose region. HRS is more prominent in the G2 phase of the cell cycle than the G0/G1 or S phases. Here I provide the first cytogenetic evidence of low-dose hyper-radiosensitivity in human peripheral blood lymphocytes using structural chromosomal aberrations. Human peripheral blood lymphocytes from two normal healthy female donors were acutely exposed to cobalt-60 gamma rays in either G0 or G2 using closely-spaced doses ranging from 0-1.5 Gy. Structural chromosomal aberrations were enumerated and the slopes of the regression lines at low doses (0-0.4

Gy) were compared with doses of 0.5 Gy and above. HRS was clearly evident in both donors for cells irradiated in G2. No HRS was observed in cells irradiated in G0. The radiation effect per unit dose was 2.5-3.5 fold higher for doses ≤0.4 Gy than >0.5 Gy**.** These data provide the first cytogenetic evidence for the existence of HRS in human cells irradiated in G2 and suggest that LNT models may not always be optimal for making radiation risk assessments at low doses.

AUTOBIOGRAPHICAL STATEMENT

ISHEETA SETH

EDUCATION:

- 2009-2014 Ph.D. in Biological Science, Wayne State University, Detroit, MI, USA
- 2005-2009 B.Tech in Biotechnology, Amity University, Noida, India

AWARDS AND HONORS:

- Thomas C. Rumble University Graduate Fellowship for the academic year 2013-2014.
- New Investigator co-chair of the Risk Assessment Special Interest Group in Environmental Mutagenesis and Genomics Society (EMGS), (2014-2016).
- Student and New Investigator Travel Award (2012, 2013) - EMGS.
- Certificate of Recognition for Exceptional Service as a GTA, 2012 - Wayne State University.
- Michigan Campus Compact 2012-2013 Heart & Soul Award, April 2013.
- Summer stipend award for 2012, Department of Biological Sciences, Wayne State University.
- First place Best Student Poster presentation award, 42nd (October 2011) annual EMS conference, Montreal, Canada.
- President - Graduate Employee's Organizing Committee (Summer 2012 - Spring 2014)

PLATFORM STYLE PRESENTATIONS AT CONFERENCES:

- Invited to present at a satellite meeting on DNA Repair/Genome Instability held during the American Society of Human Genetics (ASHG) meeting in October 2013 in Boston.
- Selected to give a platform talk in Symposium "Indirect Mechanisms of Mutagenesis: Implications for Low-Dose Risk Assessment" at the 44th Annual EMGS meeting in September 2013 in Monterey, California.
- Participated in various poster presentations (University wide, departmental, and conferences).

PUBLICATIONS (PEER-REVIEWED):

- Cheong, H.*, **Seth, I.***, Joiner, M.C., and Tucker, J.D. (*joint first authors) (2013) Relationships among micronuclei, nucleoplasmic bridges and nuclear buds within individual cells in the cytokinesis-block micronucleus assay. Mutagenesis 28:433-440.
- **Seth, I**., Schwartz, J.L., Stewart, R.D., Emery, R., Joiner, M.C., and Tucker, J.D. (2014) Neutron exposures in human cells: bystander effect and relative biological effectiveness, PLOS ONE Vol 9 (6): e98947.
- **Seth, I.**, Joiner, M.C., and Tucker, J.D. (2014) Cytogenetic low-dose hyper-radiosensitivity is observed in human peripheral blood lymphocytes (submitted).